South African Journal of Botany 180 (2025) 710–726

Contents lists available at ScienceDirect

South African Journal of Botany

journal homepage: www.elsevier.com/locate/sajb

Antimicrobial and anti-biofilm activities of the essential oils of *Lavandula angustifolia* Mill, *Salvia sclarea* L, and *Mentha pulegium* L against uropathogenic *Staphylococcus aureus in vitro* and *in silico*

Rafik Aniba[a,c,*], Amal Ramzi[b], Asmaa Dihmane[a], Habiba Raqraq[a], Amina Ressmi[a], Kaotar Nayme[c], Mohammed Timinouni[d], El idrissi Mohammed[e], Farah Abdellah[b], Abouddihaj Barguigua[a]

[a] Team of Biotechnology & Sustainable Development of Natural Resources, Department of Biology, Polydisciplinary Faculty, Sultan Moulay Slimane University, Beni Mellal, Morocco
[b] Laboratory of Applied Organic Chemistry, Faculty of Sciences and Technologies, Sidi Mohamed Ben Abdellah University, Imouzzer Street, Fez 2202, Morocco
[c] Molecular Bacteriology Laboratory, Pasteur Institute of Morocco, Casablanca, Morocco
[d] Laboratoire de Biotechnologie et bio-informatique: Ecole des Hautes Etudes de Biotechnologie et de santé (EHEB), Casablanca, Morocco
[e] Team of Chemical Processes and Applied Materials, Faculty Polydisciplinary, Sultan Moulay Slimane University, Beni-Mellal, Morocco

ARTICLE INFO

Article History:
Received 31 July 2024
Revised 19 November 2024
Accepted 18 March 2025
Available online xxx

Edited by: Dr I. Famuyide

Keywords:
Antibacterial activity
Antibiofilm activity
Essential oils
Molecular docking
Synergy
Staphylococcus aureus

ABSTRACT

The aim of this study was to explore the antimicrobial and antibiofilm activities of essential oils (EOs) obtained from *Salvia sclarea* L, *Lavandula angustifolia* Mill, and *Mentha pulegium* L, using *in vitro* and *in silico* experiments. Additionally, the study to evaluate the synergistic effects of these EOs in combination with certain conventional antibiotics against *Staphylococcus aureus* isolated from urinary tract infections.

The EOs used in this study were obtained by hydrodistillation, and their chemical compositions were analyzed using gas chromatography-mass spectrometry. Antibacterial activity was assessed using the disk diffusion method and modified broth microdilution method, whereas antibiofilm effects were evaluated using the microtiter plate biofilm formation method. The synergies effects between antibiotics with three EOs against *S. aureus* isolates were assessed using a checkerboard titration assay. The AutoDock Vina program was used to perform molecular docking and to calculate the predictive binding affinities of four major volatile compounds to five proteins essential for antibiotic resistance and biofilm formation. In addition, drug similarity properties were predicted using SwissADME, while toxicity was predicted using ProToxII.

The major components of *S. sclarea* L, *L. angustifolia* Mill, and *M. pulegium* L EOs were linalyl acetate, 1,8-cineole, and pulegone, respectively. These EOs showed excellent antibacterial activity against methicillin-susceptible and-resistant *S. aureus* strains. Surprisingly, the fractional inhibitory concentration index showed that mixing EOs with antibiotics had a significant synergistic antibacterial effect. All EOs showed potent antibiofilm activity against biofilm-forming *S. aureus* strains at subinhibitory concentrations.

Molecular docking results revealed that 1,8-cineole, camphor, linalyl acetate, and pulegone of the three EOs have significant potential to inhibit target proteins involved in adhesion, biofilm formation, and antibiotic resistance. In addition, SwissADME prediction results showed that all four components satisfied the rule of five and had acceptable drug-like characteristics.

In vitro and *in silico* studies have highlighted the EOs of *S. sclarea* L, *L. angustifolia* Mill, and *M. pulegium* L as promising natural sources of antibacterial and antibiofilm agents that could be effective in combination with antibiotic therapies, thereby minimizing the impact of antibiotic resistance and combating infectious diseases.

1. Introduction

Staphylococcus aureus is a coagulase-positive staphylococcus and a relatively uncommon cause of urinary tract infections (UTIs) in the general population, with a prevalence rates of 0.5%-6% (Yousefi et al., 2016). Nevertheless, it can be more prevalent in specific population groups, such as elderly patients with urinary catheters

* Corresponding author.
E-mail addresses: rafikaniba1466@gmail.com, rafik.anibafpb@usms.ac.ma (R. Aniba).

https://doi.org/10.1016/j.sajb.2025.03.038

or those with *S. aureus* bacteremia (Hashemzadeh et al., 2021; Rafik et al., 2021).

The global rise of multidrug-resistant (MDR) uropathogenic *S. aureus* strains represents a substantial healthcare challenge. Studies indicate that more than half of *S. aureus* strains are resistant to penicillins and cephalosporins, leading to the emergence of methicillin-resistant S. aureus (MRSA) (Hashemzadeh et al., 2021). MRSA is considered a high-priority bacterial pathogen because of its resistance to a broad range of commonly used antibiotics, such as tetracyclines, macrolides, aminoglycosides, and fluoroquinolones (Piechota et al., 2018). MRSA infections, including UTIs, are associated with high morbidity and mortality owing to their ability to produce a multitude of virulence factors that contribute to bacterial invasion, including those involved in adhesion and biofilm formation (Manandhar et al., 2018).

Biofilm formation is a key factor in the persistence of over 80% of infections, including UTIs (Piechota et al., 2018). The biofilm matrix created by *S. aureus* facilitates cell to cell interactions and promotes the horizontal transfer of resistance and virulence genes, exacerbating the spread of these traits (Águila-Arcos et al., 2017). These biofilms present a critical obstacle to treatment, as bacteria within biofilms exhibit increased tolerance to antimicrobial agents compared with planktonic forms (Águila-Arcos et al., 2017).

Given these challenges, researchers are investigating novel therapeutic approaches to mitigate *S. aureus* resistance and to manage biofilm formation. Among these emerging strategies, phytotherapy based on natural antimicrobials, such as essential oils (EOs), has garnered attention. EOs are secondary metabolites of aromatic plants and are utilized in various fields, including aromatherapy, food preservation, and medicine. Notably, recent studies have demonstrated the antimicrobial properties of EOs, with findings indicating that they can inhibit or eradicate a wide range of bacterial pathogens (Bolouri et al., 2022). While there is substantial evidence supporting the efficacy of EOs against planktonic bacteria (Abers et al., 2021; Iseppi et al., 2020), fewer studies have explored their impact on biofilm-embedded bacteria or their ability to eliminate bacterial adhesion on surfaces (Cutro et al., 2023; Walsh et al., 2019).

This gap underscores a significant research challenge: While EOs have shown promise, their antibiofilm activity, especially against MDR pathogens such as *S. aureus*, remains underexplored. The novelty of recent studies lies in their examination of EOs not only as bactericidal agents, but also as potential disruptors of biofilm integrity, which could offer alternative therapeutic strategies in the era of rising antimicrobial resistance.

Our study builds on these findings by evaluating the antimicrobial and antibiofilm activities of EOs derived from *Lavandula angustifolia* Mill, *Salvia sclarea* L, *and Mentha pulegium* L against *S. aureus* strains. Additionally, we investigated the potential synergistic effects of these EOs when combined with conventional antibiotics (gentamicin, vancomycin, and ciprofloxacin) to enhance their efficacy. We conducted an *in silico* analysis to predict the mechanisms of action of EOs components using molecular docking and absorption, distribution, metabolism, excretion, and toxicity (ADMET) profiling, offering insights into their possible roles in antibiofilm and antimicrobial activities.

2. Materials and methods

2.1. Plant material

Aerial parts (leaves, stems, and flowers) of *L. angustifolia* Mill, *M. pulegium* L, and *S. sclarea* L were collected from the Taounate region of Morocco. The plants were harvested at the flowering stage in accordance with the AFNOR standard (2000) (Didier, 2000), and the guidelines published by Lkhoumsi et al., on good collection practices for aromatic and medicinal plants (Lkhoumsi et al., 2004). Botanical identification of the three species was carried out at the National Institute of Medicinal and Aromatic Plants, Sidi Mohamed Ben Abdellah University, Fez, Morocco. Authenticated voucher specimens (USMBA/L-22/023 for *L. angustifolia* Mill, USMBA/M-22/026 for *M. pulegium* L and USMBA/S-22/028 for *S. sclarea* L) have been placed in the herbarium of this institute.

2.2. Extraction of EOs

The hydro-distillation method was used to extract the EOs. First, the plants were air dried at room temperature. One hundred grams (100 g) of the each dried sample was submitted to extraction for three hours using a Clevenger apparatus, following the method described in the European Pharmacopoeia (Council of Europe, European Pharmacopoeia Commission, 2007). This method is highly recommended for the extraction of EOs, as it is a simple, faster, low-cost method in comparison to the other extraction techniques with low cost and has minimum environmental impact compared to other extraction techniques. It also allows for a high yield and recovery of the EO compounds (Ma et al., 2023). The EOs were then collected in vials containing anhydrous sodium sulphate (0.5−2 g) and stored at 4°C in dark glass vials until further use. The yields of the EOs extracted from the different plants were calculated based on dry biomass. All the extractions were performed in triplicate.

2.3. Chemical analysis

Gas chromatography coupled with mass spectrometry (GC-MS) was used to identify the chemical compounds in the studied EOs. The analysis was performed using a Shimadzu (TQ-8040) series GC-MS system (Shimadzu, Tokyo, Japan) equipped with an AOC-20i Plus auto-injector. The column used was a Rxi-5MS capillary column (30 m × 0.25 mm i.d., 0.25 μm). The oven temperature was initially programmed at 50 °C for 5 min, then increased to 250 °C at a rate of 4 °C/min, and maintained isotherm for 10 min. The injector and detector temperatures were maintained at 280°C, with helium was used as the vector gas at a flow rate of 1.4 mL/min. Electron impact ionization was applied with an ionization energy of 70 eV. The GC-MS Solution ver.4 software (Shimadzu, Tokyo, Japan) was used to manage the system, set the parameters for both the GC and mass spectrometry, collect data, and process it.

The compounds were identified by a comparing of their mass spectra with data from the 11th Edition of NIST 2017 and the Adams terpene library (Adams, 2017). Each analysis was conducted in triplicate.

2.4. S. aureus isolates

The *S. aureus* strains used in this study included two ATCC strains (ATCC 25923 and ATCC 43300, American Type Culture Collection, Manassas, Virginia, USA) and 20 non-duplicated uropathogenic strains forming biofilm, which include MRSA (n = 9) and MSSA (n = 11). Following hierarchical clustering analysis, these clinical strains were grouped into four categories based on antibiotic resistance, genes associated with biofilm formation, and biofilm formation intensity. The phenotypic and genotypic characteristics of the clinical strains are summarized in Table 1 and have been previously published (Aniba et al., 2024).

2.5. Screening for antibacterial activity of EOs

2.5.1. Agar disk diffusion

The antibacterial activity of EOs was evaluated using the disk diffusion method, as described previously (Mollea et al., 2022). After inoculating *S. aureus* strain (0.5 McFarland) onto the surface of a Mueller-Hinton plate (Bio-Rad, Marnes-la-Coquette, France), sterilized discs (6 mm in diameter) impregnated with 10 μL of each EO

Table 1
Phenotypic and genotypic characteristics of antibiotic resistance and biofilm formation in the S. aureus strains used in this study.

Group	Strain	Methicillin resistance	Resistance pattern[Δ]	Biofilm formation ability	Genotypic profile of biofilm production[*]
Group 1	Usa 300822	MSSA	P, Te	Weak	Genotype 6
	Usa 080421		P, FA, Vn, Tei	Moderate	Genotype 2
	Usa 210321		P, FA		Genotype 3
	Usa 150421		P, E, Te, FA, Vn, Tei, F		
	Usa 161121		P, Te		
	Usa 260322		P, Te, F		Genotype 5
	Usa 040521		P, FA	Strong	Genotype 1
	Usa 181121		P, E, CL		Genotype 3
	Usa 180222		P, Te		Genotype 4
Group 2	Usa 101121	MRSA	P, Te	Moderate	Genotype 7
	Usa 010422		P, Te		Genotype 8
	Usa 220822		P, Te	Strong	
Group 3	Usa 271221		P, Tm, E, Te, Tg, FA, Vn, Tei, F, CL	Moderate	Genotype 8
	Usa 200422		P, E, Te, FA, F, CL		
	Usa 060722		P, E, Te, FA, Tei, F	Strong	Genotype 8
	Usa 220321		P, Tm, G, E, Te, Tg, FA, Tei, F, Le		Genotype 4
Group 4	Usa 080722		P, Tm, G, E, FA, SXT, F	Weak	Genotype 8
	Usa 210921		P, Tm, E, Te, Tg, FA, F, CL	Moderate	Genotype 4
	Usa 191121		P, Tm, G, E, Te, Tg, FA, Tei, F, Le		Genotype 9
	Usa 290822		P, Tm, G, E, Tei, FA, F, Le	Strong	Genotype 8

Δ P: Penicillin G; FA: Fusidic Acid; Te: Tetracycline; E: Erythromycin; F: Fosfomycin; Tm: Tobramicin; Tei: Teicoplanin; G: Gentamicin; CL: Clindamycin; Tg: Tigecycline; Le: Levofloxacin; Vn: Vancomycin; SXT: Trimethoprim-sulfamethoxazole; Ln: Linezolid.
[*]Genotype 1: *spa, clfA, fnbB, icaR*; Genotype 2: spa, clfA, fnbB,bap, icaA, icaR; genotype 3: spa, clfA, fnbB, bap, fnbA, icaA, icaR; Genotype 4: *spa, clfA, fnbB, bap, fnbA, icaA, icaB; Genotype 5: spa, clfA, fnbB, bap, fnbA*; Genotype 6: *spa, clfA, fnbB, bap, fnbA, icaA*; Genotype 7: *spa, clfA, fnbB, bap, fnbA, icaA, icaB, icaR*; Genotype 8: *spa, clfA, fnbB, bap, fnbA, icaA, icaB, icaD;* Genotype 9: *spa, clfA, fnbB, bap, fnbA, icaA, icaB, icaD, icaR*

were placed on the plate (The EO stock concentration was 1000 mg/mL). Gentamicin disks (10 μg) and disks containing 10 μL of dimethyl sulfoxide 1% (v/v) (DMSO) were used as the positive and negative controls, respectively. After incubation at 35±2°C for 20± 4h, the inhibition zone diameter (IZD) of each EO was measured and interpreted using the following criteria: no activity, IZD less than 6 mm; weak activity, IZD between 6 and 12 mm; moderate activity, IZD between 12 and 20 mm; strong activity, IZD greater than 20 mm. All experiments were conducted in triplicate.

2.5.2. The modified broth microdilution method

The minimum inhibitory concentration (MIC) and the minimum bactericidal concentration (MBC) of the selected EOs were determined using the Clinical and Laboratory Standards Institute (CLSI) guidelines to evaluate their antibacterial activities against all *S. aureus* isolates (CLSI, 2018).

With some modifications, the resazurin-based 96-well plate microdilution method was used to determine the EOs' MICs (Elshikh et al., 2016). A 96-well microtiter plate containing 88 μL of Muller Hinton broth (MHB, Oxoid, Thermo Scientific^{TM}) was used to prepare serial dilutions of EOs ranging from 16 to 0.0062 mg/mL. To ensure solubility in the culture medium, 1% (v/v) DMSO was added. We grew the isolates on mannitol salt agar (MSA, Biokar Diagnostics, Beauvais, France) agar media and incubated them at 35±2°C for 20± 4h. We then adjusted the concentration to 0.5 McFarland (10^8 colony-forming units (CFU)/mL) and added 10 μL to each well to get a final concentration of 5×10^5 CFU/mL per well. Under aerobic conditions, the microtiter plates were incubated at 35±2°C for overnight. Then, 5 μL of a 1% aqueous resazurin solution (Sigma, Darmstadt, Germany) was put into each well and left to sit for two hours at 35± 2°C. The appearance of a red color was used to determine bacterial growth.

The MBC was determined in wells containing extract concentrations with no visible bacterial growth. Ten microliters of each well were inoculated on MSA agar medium and incubated at 35±2°C for 20±4h. The MBC was defined as the lowest concentration of EOs needed to eliminate 99.9% of the bacteria examined (no visible colonies). All tests were performed in triplicate, and gentamicin (Sigma-Aldrich, St. Louis, MO, USA) was used as a positive control.

To determine the effect of EOs, the MBC/MIC ratio was calculated. If the MBC/MIC ratio was less than 4, the EO was considered bactericidal. If the MBC/MIC ratio was greater than 4, the EO was considered bacteriostatic (Jaber et al., 2021).

2.6. Determination of pharmacodynamical interaction between EOs in combination with antibiotics

2.6.1. Choice of antibiotics and EOs

The selection of antibiotics was based on the list provided by the CLSI recommendations (CLSI, 2018) and the availability of these drugs during laboratory handling. One antibiotic from each family (aminoglycosides, fluoroquinolones, and glycopeptides) was selected. Gentamicin, levofloxacin and vancomycin were purchased from Sigma Aldrich (St. Louis, MO, USA) and tested at different concentrations in accordance with CLSI recommendations for each drug family. *L. angustifolia* Mill, *S. sclarea* L, and *M. pulegium* L EOs were chosen to study their interaction with antibiotics because of their high antimicrobial potential against *S. aureus* strains, as well as the availability of sufficient quantities during the tests.

2.6.2. Checkerboard assay

A checkerboard titration assay was performed to evaluate the susceptibility of *S. aureus* isolates to mixtures of an antibiotic (gentamicin, levofloxacin, and vancomycin) and three EOs (*L. angustifolia* Mill, *S. sclarea* L, and *M. pulegium* L) against four clinical isolates. The fractional inhibitory concentration index (FICI) was determined as described in a previous study (Sreepian et al., 2022). Briefly, various concentrations of EOs, ranging from 16 to 0.0062 mg/mL, were prepared by serial dilution in sterile tubes. Similarly, different concentrations of antibiotics were prepared, ranging from 0.0062 to 16 μg/mL. One hundred microliters of each EO, tested in combination with antibiotics (v/v) at different concentrations, were added to the wells. Ten microliters of bacterial inoculum (10^5 CFU/mL) were added to each

well of the microtiter plates. Under aerobic conditions, the microtiter plates were incubated at 35±2°C for 20±4h.

The FICI was calculated using the following formula:

$$FICI = \frac{MIC_{EOcombination}}{MIC_{EO\ alone}} + \frac{MIC_{ATB\ combination}}{MIC_{ATB\ alone}}$$

$MIC_{EO\ combination}$: MIC of EO in combination; $MIC_{EO\ alone}$: MIC of EO alone; $MIC_{ATB\ combination}$: MIC of antibiotic in combination; $MIC_{ATB\ alone}$: MIC of antibiotic alone.

The results were analyzed according to the following FICI criteria: The combination was considered synergistic when FICI $\leq$ 0.5, additive when 0.5 $<$ FICI $\leq$ 1, indifferent when 1 $<$ FICI$\leq$ 2 et antagonistic when FICI $\geq$ 2 (Sreepian et al., 2022).

2.7. Anti-biofilm activity

All biofilm-forming *S. aureus* isolates were selected to test the ability of EOs to inhibit biofilm formation using the microtiter plate biofilm formation method. The experiment was conducted on sterile 96-well polystyrene plates. The strains were incubated with EOs at MIC/2, MIC/4, MIC/8, and MIC/16, supplemented in brain heart infusion broth (Oxoid, Thermo Scientific™) and 1% DMSO, at 35±2 °C for 48h without agitation. A negative control well, containing neither EOs nor bacteria, was included. After incubation, biofilm formation was quantified using 1 % crystal violet staining. The tests were performed three times. An automatic micro-ELISA reader (BioTek EL x 800, USA) was used to measure the optical density (OD) of adherent and stained bacteria by measuring absorbance at 590 nm.

The formula used to calculate the percentage inhibition of biofilm formation was determined as follows (Morshdy et al., 2022):

$$\text{Inibition biofilm formation } (\%) = \frac{ODc - ODt}{ODc} \times 100$$

ODc: Optical density of the biofilm formed without EOs.
ODt: Optical density of biofilm formation in the presence of an EO.

2.8. Molecular docking analysis of the main identified compounds

Molecular docking was used to investigate the binding energy and mechanism, and to predict the toxicity of the major constituents extracted from EOs, as well as several common antibacterial targets (Fig. 1).

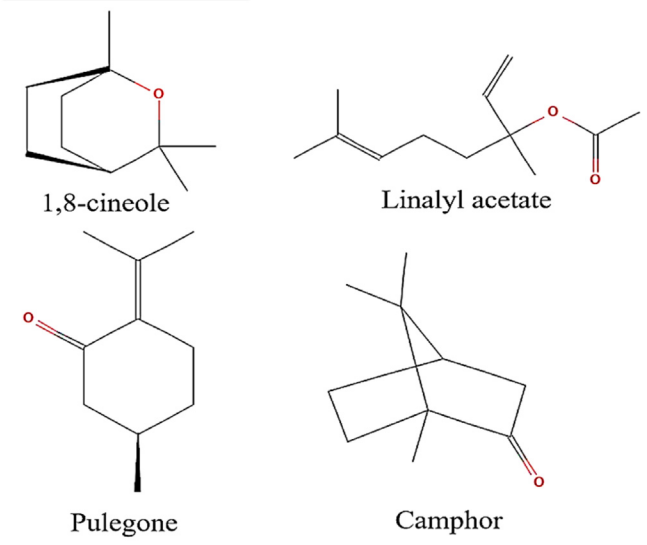

Fig. 1. Chemical structures of the major components of L. angustifolia Mill (1,8-cineole et camphor), S. sclarea L (linalyl acetate), and M. pulegium L (pulegone) EOs.

2.8.1. Protein preparation

Seven *S. aureus* proteins were targeted in this study: penicillin-binding protein (PLP2a), responsible for methicillin resistance, and several proteins involved in adhesion and biofilm formation, including biofilm-associated protein (Bap), fibronectin-binding protein A and B (FnbA and B), clumping factor A (ClfA), intercellular adhesion proteins (IcaA, IcaB, and IcaD), and poly-β (1,6)-*N*-acetyl-D-glucosamine (PNAG). The crystal structure of these proteins were retrieved from the RCSB Protein Data Bank (RCSB PDB) (https://www.rcsb.org/) and downloaded as a PDB file with the following PDB IDs: PLP2a (PDP ID: 1VQQ), Bap (PDB ID: 7C7U), FnbA (PDB ID: 2RKZ), FnbB (PDB ID: 2RKZ), ClfA (PDB RID: 1N67), IcaA (PDB ID:4P7R), IcaB (PDB ID: 4WCJ), IcaD (PDB ID:1F2R), and PNAG (PDB ID:7T8N).

All protein structures were prepared by removing original inhibitors and water molecules. Energy minimization was performed prior to docking simulation using the PyMOL 3.0 (Schrödinger, Portland, USA) and AutoDock Tools of the Vina program. The protein structures were then saved in the PDBQT format for further analysis.

2.8.2. Ligand preparation

The crystal structures of four major chemical compounds identified in the *L. angustifolia* Mill, *S. sclarea* L, and *M. pulegium* L EOs (1,8-cineol, camphor, linalyl acetate, and pulegone) were retrieved from the PubChem database (https://pubchem.ncbi.nlm.nih.gov/). Their three-dimensional (3D) structure was downloaded in the SDF format and converted into the Protein Data Bank (PDB) format by using PyMOL. AutoDock Tools was used to convert the ligands into the PDBQT format, preparing them for molecular docking simulations.

2.8.3. Molecular docking analysis of the isolated compounds

Molecular docking analysis of all selected phytocompounds against bacterial receptors was conducted using AutoDock Vina software. The PDBQT ligands were docked into the receptor binding sites using AutoDock Vina's standard parameters. The Vina Score, representing the predicted binding free energy (kcal/mol), was calculated and analyzed. To identify hydrogen bonds, BIOVIA Discovery Studio Visualizer (San Diego, CA, USA, 2021) was used, and the interacting residues were visualized in the ball-and-stick model.

2.8.4. Drug-likeness

Drug likeness, physicochemical and pharmacokinetic characteristics, as well as ADME analysis of the selected phytocompounds were carried out using SwissADME software (http://www.swissadme.ch/). The 3D structures of the shortlisted compounds were obtained in canonical simplified molecular input line entry system (SMILES) format from the PubChem database and uploaded to SwissADME for analysis.

2.8.5. Toxicity prediction

The Pro-Tox-II webserver tool (https://tox-new.charite.de/protox3/) was used to predict the toxicity class and the predicted median lethal dose (LD50in mg/kg body weight) of the four ligands.

2.8.6. Statistical analysis

Data were collected using a Microsoft Excel spreadsheet (Microsoft Corp., Redmond, WA, USA, 2016), and analyzed with IBM SPSS Statistics 26 (IBM, Armonk, NY, USA). The antibacterial activity for the EOs data was analyzed using Dunnett's test, while, data on the biofilm formation inhibition were compared using the nonparametric Kruskal-Wallis test. Statistical significance was set at $p \leq 0.05$.

3. Results

3.1. Extraction yield and chemical characterization

The yield of EOs varied between plants. The extraction of *L. angustifolia* Mill resulted in a yield of 3.20±0.14%, *Salvia sclarea* L yielded 1.98± 0.61%, and *Mentha pulegium* L provided 2.5 ± 0.23%. GC-MS analysis revealed chemical variability among the tested EOs (Supplementary Table 1).

Nineteen chemical compounds were identified in the *L. angustifolia* Mill EO, accounting for a total of 98.24±0.2%. This EO was rich in oxygenated monoterpenes (88.44±0.13%), with the ether compound 1,8-cineole being the major constituent (50.8±0.19%), followed by camphor, a ketone (18.12±0.45%).

In the *S. sclarea* L EO, ten compounds were identified, representing 97.28±0.10% of the total composition. This EO was also rich in oxygenated monoterpenes (90.25±0.16%), with hydrocarbon compounds accounting for only 5.53±0.14%. The most abundant constituent was the monoterpene ester linalyl acetate (63.62±0.2%), followed by camphor (11.44±0.16%), and linalool (9.6±0.1%).

For the *M. pulegium* L EO, 18 compounds were identified, representing 98.9±0.18%. GC-MS analysis revealed a predominance of oxygenated monoterpenes (94.09±0.21%), with the monoterpene ketone pulegone being the main bioactive constituent (73.33±0.18%), followed by piperitenone (11.81±0.12%) and cis-isopulegone (3.16± 0.31%).

3.2. Antibacterial properties of L. angustifolia Mill, S. sclarea L, and M. pulegium L

The *in vitro* antibacterial activity results of the three EOs against *S. aureus* isolates using the disk diffusion method are summarized in Table 2. The results are expressed as IZD, which depends on the EOs examined and the sensitivity of the different strains tested to the EOs. In the current study, 15% of *S. aureus* strains were most sensitive to *L. angustifolia* Mill, with an IZD greater than 20 mm, followed by 65% of strains that were moderately sensitive to an IZD between 6 and 12 mm. However, 20% of the strains showed low sensitivity. Additionally, *S. sclaree* L showed moderate and low antibacterial activity against *S. aureus* strains of 25% and 75%, respectively.

M. pulegium L exhibited moderate antibacterial activity against 75% of *S. aureus* strains, with IZDs between 6 and 12 mm. The IZDs of *L. angustifolia* Mill. and *M. pulegium* L EOs were significantly greater against MSSA strains than against MRSA ($p \leq 0.05$) (Figs. 2 and 3).

The results obtained from the disk diffusion test were confirmed by the quantitative antibacterial effects of EOs (MBC and MIC) (Table 3). The MICs obtained in our experiments were between 0.5 and 4 mg/mL, 4 and 16 mg/mL, and 0.5 and 16 mg/mL for *L. angustifolia* Mill, *S. sclarea* L, and *M. pulegium* L EOs, respectively. *S. sclarea* L and *M. pulegium* L EOs had a bactericidal effect on 90% of *S. aureus* strains. In contrast, *L. angustifolia* Mill EO showed a bacteriostatic effect against 60% of *S. aureus* strains and a bactericidal effect against 40% of the strains.

The MICs of *L. angustifolia* Mill and M. pulegium EOs were significantly lower against MSSA strains than those of MRSA ($p \leq 0.05$) (Fig. 4).

The antibacterial properties of *L. angustifolia* Mill, *S. sclarea* L, and *M. pulegium* L in relation to phenotypic and genotypic traits of antibiotic resistance and biofilm formation in *S. aureus* indicated that *S. aureus* group 1 was highly sensitive to *L. angustifolia* Mill and *M. pulegium* L EOs, with an average IZD of 16.9 mm and 13 mm, respectively ($p \leq 0.05$), and with an average MIC value of 0.94 mg/mL and 1.94 mg/mL, respectively ($p \leq 0.05$) (Figs. 5 and 6).

3.3. Antibacterial activity of antibiotics in combination with EOs

The *L. angustifolia* Mill EO showed synergistic interactions with gentamicin and vancomycin against all the tested *S. aureus* strains (U*sa*210921 MRSA: “gentamicin” FICI=0.25; “vancomycin” FICI=0.375; U*sa*101121 MRSA: “gentamicin” FICI=0.375; “vancomycin” FICI=0.282; U*sa*220321 MSSA: “gentamicin” FICI=0.313; “vancomycin” FICI=0.156; U*sa*260322 MSSA: “gentamicin” FICI=0.281; “vancomycin” FICI=0.313).

Similarly, we observed a synergistic effect in the following combinations: the *S. sclarea* L EO with gentamicin against three *S. aureus* strains (U*sa*101121 MRSA: FICI=0.375; U*sa*220321 MSSA: FICI=0.313; and U*sa*260322 MSSA: FICI=0.376), the *S. sclarea* L EO with levofloxacin against two MSSA isolates (U*sa*220321 MSSA: FICI=0.267; and U*sa*101121 MSSA: FICI=0.375), and the *S. sclarea* L EO with vancomycin against all tested *S. aureus* isolates (U*sa*101121 MRSA: FICI=0.25;

Table 2
Antimicrobial effects of L. angustifolia Mill, S. sclarea L, and M. pulegium L EOs.

EOs	L. angustifolia Mill		S. sclarea L		M. pulegium L		Gentamicin	
Strains	IZD (mm)	MBC (mg/mL)/ MIC (mg/mL)	IZD (mm)	MBC (mg/mL)/ MIC (mg/mL)	IZD (mm)	MBC (mg/mL) / MIC (mg/mL)	IZD (mm)	MBC (mg/L) / MIC (mg/L)
Usa 220321	12±1	8/1	8±0.5	16/2	8±0.5	4/2	10±0.5	32/16
Usa 040521	10±1.5	4/1	8±0.5	16/8	12±1	4/0.5	22±1	2/1
Usa 080421	16±0.5	4/1	11±1	16/8	14±1.75	8/4	26±1	0.5/0.25
Usa 210321	16±1	8/1	11±2	8/4	15±1.5	4/2	30±2	0.5/0.25
Usa 150421	21±0.75	2/1	10±1.75	8/4	14±0.5	4/2	26±0.5	0.5/0.25
Usa 210921	10±1	16/4	10±1	16/8	12±1	16/8	24±1	0.5/0.25
Usa 101121	12±0.5	8/2	8±0.5	16/8	12±0.5	4/2	26±1	1/0.5
Usa 191121	16±0.5	16/4	11±1	32/16	10±1.75	16/8	12±0.5	64/16
Usa 161121	16±1	8/1	15±2	16/8	12±1.5	8/4	28±1	1/0.5
Usa 181121	22±0.75	2/1	8±1.75	16/2	14±0.5	4/2	30±1.5	0.5/0.25
Usa 271221	10±1	8/1	10±1	8/4	12±1	4/2	26±0.5	0.5/0.25
Usa 010422	12±0.5	8/1	10±0.5	8/4	12±0.5	4/2	24±1	2/1
Usa 180222	15±1	8/1	12±0.5	8/4	10±0.5	2/0.5	22±1	0.5/0.5
Usa 260322	15±0.5	8/1	10±0.5	16/8	12±0.75	4/2	20±0.5	0.5/0.5
Usa 200422	14±1	8/1	12±1.5	16/8	8±1	4/2	28±1.5	1/0.5
Usa 060722	10±1.15	8/1	12±0.75	16/4	12±0.5	16/4	30±2	0.5/0.25
Usa 080722	12±0.5	16/2	11±0.5	16/8	10±2	32/16	8±1	64/16
Usa 220822	16±0.5	8/1	10±0.75	8/4	12±1	8/4	24±1	2/1
Usa 290822	14±0.5	16/4	8±1	16/8	12±0.5	8/4	10±1	64/16
Usa 300822	21±1	4/0.5	14±0.5	16/4	14±0.5	4/0.5	24±0.5	2/1
ATCC43300	12±0.5	8/2	10±0.5	16/8	10±0.5	4/2	8±0.5	>64/16
ATCC25923	21±0.75	2/1	10±1.75	8/4	14±0.5	4/2	22±1	1/1

MIC: Minimum inhibitory concentration; MBC: Minimum bactericidal concentration; IZD: Inhibition zone diameter; EO: Essential oil

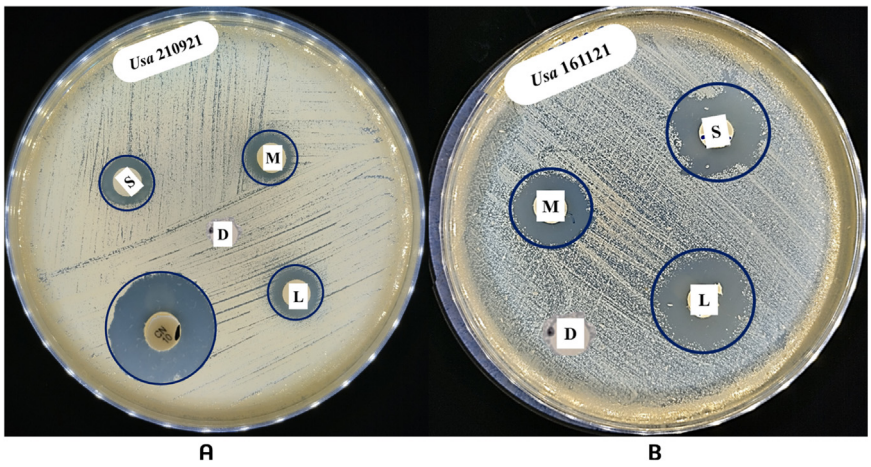

Fig. 2. Zone of inhibition (mm) of L. angustifolia Mill (M), S. sclarea L (S), M. pulegium L (**M**), gentamicin (**GN**), and dimethyl sulfoxide (1%) (**D**) against uropathogenic *S. aureus* on Mueller Hinton agar. U*sa* 161121 MSSA (**A**) and U*sa* 210921 MRSA (**B**).

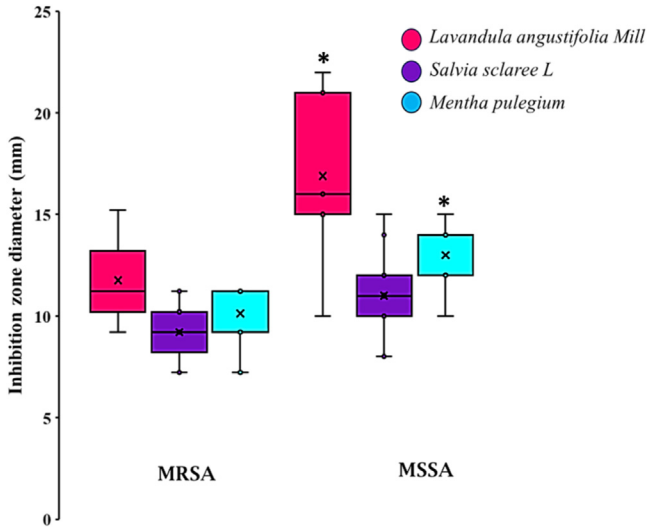

Fig. 3. Antibacterial activity of EOs was determined by disc diffusion assays. Significance was determined using the Dunnett's test. * p≤ 0.05, ** p≤ 0.01, *** p≤ 0.001.

U*sa*101121 MRSA: FICI=0.258; U*sa*220321 MSSA: FICI=0.375, and U*sa*260322 MSSA: FICI=0.258).

Additionally, there was an additive effect for the combination of the *M. pulegium* L EO and gentamicin against the tested MRSA strains (U*sa*210921 MRSA and U*sa* 101121 MRSA: FICI=0.5), while a synergistic effect for the tested MSSA (*Usa*220321 MSSA: FICI=0.313, and U*sa*260322 MSSA: FICI=0.375) (Table 3). Based on the checkerboard method, there were no antagonistic interactions when combining of the three EOs and conventional antibiotics.

3.4. Antibiofilm properties of EOs

We analyzed the antibiofilm activity of the *L. angustifolia* Mill, *S. sclarea* L, and *M. pulegium* L EOs separately against *S. aureus* strains at various concentrations (MIC, MIC/2, MIC/4, MIC/8, and MIC/16). The presence of each EOs reduced biofilm formation on polystyrene surfaces in all strains. Additionally, the effect of each EOs on biofilm formation diminished as the concentration decreased (in a dose-dependent manner). At MIC, MIC/2, MIC/4, MIC/8, and MIC/16 concentration, *L. angustifolia* Mill, *S. sclarea* L, and *M. pulegium* L EOs were found to disrupt the biofilm biomass compared with the control (Table 4). It is interesting to note that the three EOs evaluated in this study showed a greater reduction in the biofilm formation of *S. aureus* strains than gentamicin (Table 4).

Furthermore, treatment with MIC/2, MIC/4, and MIC/8 of *L. angustifolia* Mill, *S. sclarea* L and *M. pulegium* L EOs significantly reduced biofilm formation compared with untreated *S. aureus* (Fig. 7).

The antibiofilm properties of *L. angustifolia* Mill, *S. sclarea* L, and *M. pulegium* L EOs in relation to the phenotypic and genotypic traits of antibiotic resistance and biofilm formation in *S. aureus,* clearly demonstrated that these EOs reduced biofilm formation on polystyrene surfaces for all strains, regardless of their antibiotic resistance profiles or biofilm formation characteristics (Table 5).

3.5. Molecular docking

The two-dimensional (2D) and (3D) interaction patterns of the receptor-ligand complexes revealed significant binding interactions between the ligands and the receptor binding site. The *In silico* docking results showed that for PLP2a, several amino acids were involved in interactions with the ligands. Specifically, 1.8-cineole formed alkyl interactions with Leu34, Ile120, Leu124, and Val37, while camphor interacted with Val37 and Leu34, and pulegone formed interactions with Leu89 and Ala129 (Fig. 8). The stability of pulegone within the binding site is enhanced by Pi-sigma interactions with Phe133, which facilitate charge transfer and help stabilize the ligand within the PLP2a receptors (Fig. 8).

As shown in Fig. 9 (C), the oxygen atoms of pulegone and camphor participate in hydrogen bonding with Gln203 of the FnbB protein, while 1,8−cineole engages in hydrophobic (Pi-Alkyl) interactions with Tpr237. Camphor forms three Pi-alkyl bonds with Ala409, Trp518, and Val411 in ClfA protein, as well as additional Pi-sigma interactions with Trp52 (Fig. 9 (B)). Pulegone interacts with the Bap protein via a conventional hydrogen bond with DG13 and two Pi-alkyl bonds with DT11 and DC12. Camphor also interacts with the Bap protein through two conventional hydrogen bonds with DC6 and D5 (Fig. 9 (A)).

Docking analysis further revealed that pulegone forms a Pi-sigma binding interaction with the active site of the IcaB protein via Tyr74, while 1,8−cineole interacts with IcaB protein through Pi-alkyl interaction via Tyr (Fig. 10 (B)). For the IcaA protein, four amino acids (Leu7, Phe4, Tyr310, and Val307) interact with 1,8−cineole, while camphor interacts with three amino acids (Tyr181, Ile185, and Pro164) (Fig. 10 (A)).

As depicted in Fig. 10 (C), 1,8−cineole forms two Pi-alkyl bonds with Phe24 and 86 and one conventional hydrogen bond with Ser89 in the IcaD protein. Camphor binds to the IcaD protein via a single

Table 3
Activity of L. angustifolia Mill, S. sclarea L, and M. pulegium L EOs in combination with gentamicin, vancomycin, and levofloxacin against selected S. aureus strains.

Antibacterial Agent	FICI: Fractional inhibitory concentration index					
	L. angustifolia Mill	**Type of Interaction**	S. sclarea L	**Type of Interaction**	M. pulegium L	**Type of Interaction**
Usa 210921 MRSA						
Gentamicin	0.250	Synergistic	0.625	Additive	0.50	Additive
Levofloxacin	0.375	Synergistic	0.5	Additive	0.375	Synergistic
Vancomycin	0.375	Synergistic	0.25	Synergistic	0.25	Synergistic
Usa 101121 MRSA						
Gentamicin	0.375	Synergistic	0.375	Synergistic	0.50	Additive
Levofloxacin	0.2675	Synergistic	0.502	Additive	0.315	Synergistic
Vancomycin	0.282	Synergistic	0.258	Synergistic	0.282	Synergistic
ATCC 43300						
Gentamicin	0.282	Synergistic	0.375	Synergistic	0.531	Additive
Levofloxacin	0.375	Synergistic	0.375	Synergistic	0.313	Synergistic
Vancomycin	0.258	Synergistic	0.284	Synergistic	0.258	Synergistic
Usa 220321 MSSA						
Gentamicin	0.313	Synergistic	0.313	Synergistic	0.313	Synergistic
Levofloxacin	0.531	Additive	0.267	Synergistic	0.284	Synergistic
Vancomycin	0.156	Synergistic	0.375	Synergistic	0.313	Synergistic
Usa 260322 MSSA						
Gentamicin	0.281	Synergistic	0.376	Synergistic	0.375	Synergistic
Levofloxacin	0.313	Synergistic	0.375	Synergistic	0.313	Synergistic
Vancomycin	0.313	Synergistic	0.258	Synergistic	0.282	Synergistic
ATCC 25923						
Gentamicin	0.313	Synergistic	0.313	Synergistic	0.376	Synergistic
Levofloxacin	0.156	Synergistic	0.267	Synergistic	0.284	Synergistic
Vancomycin	0.258	Synergistic	0.375	Synergistic	0.282	Synergistic

conventional hydrogen bond with Ser89 and a single Pi-sigma bond with Phe24.

Additionally, 1–8 cineole forms four Pi-alkyl interactions with the active site of the PNAG protein, involving Trp318, Phe240, Trp314, and Arg237. In contrast, camphor binds to the PNAG active site through three Pi-alkyl bonds (Phe240, His342, and Arg237) and a Pi-sigma bond with Tyr317 (Fig. 11).

3.6. ADMET and drug-likness prediction

The absorption, distribution, metabolism, excretion, and toxicity (ADMET) properties of a drug are crucial factors for therapeutic use in living organisms. To assess the drug-likeness of the four major compounds in *L. angustifolia Mill, S. sclarea*, and *M. pulegium* EOs, we applied Lipinski's five rules. According to these rules, ligands should have a partition coefficient (log P) ≤5, fewer than 10 hydrogen bond acceptors, fewer 5 hydrogen bond donors, and no more than one violation of the rules. Additional molecular parameters, such as the log P and topological polar surface area (TPSA), can be used to predict the oral bioactivity of compounds.

The *in silico* analysis of the selected ligands showed good compliance with Lipinski's rules (Table 6), indicating they were soluble and lipophilic. The log P values for the four compounds 1,8–cineole, camphor, linalyl acetate, and pulegone were 2.67, 2.37, 3.24, and 2.62, respectively. All the ligands, except for linalyl acetate (TPSA: 26.3 A^2), had a TPSA value of less than 20 A^2. Additionally, all selected compounds predicted to have excellent gastrointestinal, high absorption (bioavailability score: 0.55), and were not likely to cross the blood-brain barrier. None of the compounds were found to be substrates for P-glycoprotein, suggesting that they are likely to be well absorbed in the body.

Toxicity predictions that all the ligands were non-toxic to organs, with toxicity class values ranging from 4 to 6 (Table 7). The predicted LD50 values for 1,8–cineole, camphor, linalyl acetate, and pulegone were 2480, 775, 12,000, and 470 mg/kg, respectively.

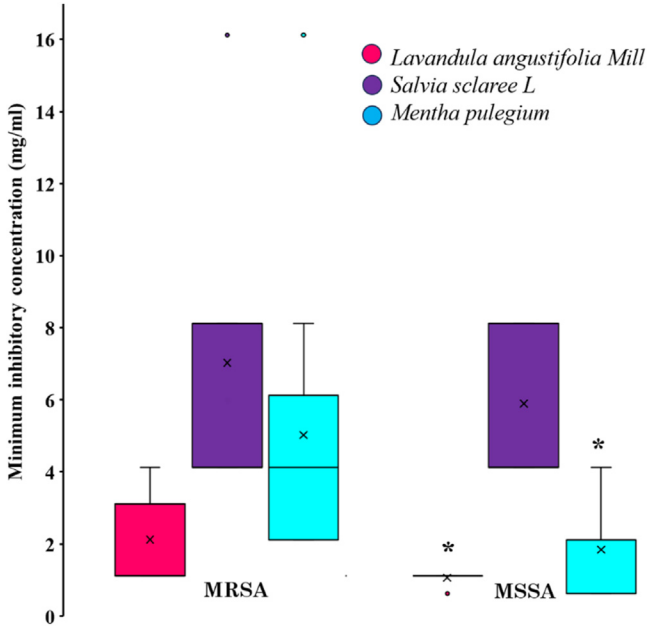

Fig. 4. MICs of EOs against MRSA and MSSA using the Modified Broth Microdilution Method. Significance was determined using Dunnett's test. * p≤ 0.05, ** p≤ 0.01, *** p≤ 0.001.

3.7. Boiled-egg

The drug-like properties and gastrointestinal absorption of the selected compounds; 1,8-cineole, camphor, linalyl acetate, and pulegone from *L. angustifolia Mill, S. sclarea* L, and *M. pulegium* L EOs were assessed by using the boiled-egg prediction (Fig. 12) and bioavailability radar graph (Fig. 13). All compounds fell within the yellow region, indicating good permeability across the blood-brain barrier, human gastrointestinal absorption, and high bioavailability.

4. Discussion

Numerous scientific studies have demonstrated that the overuse and misuse of antibiotics have led to the development of antibiotic-resistant bacteria, complicating the treatment of infectious diseases

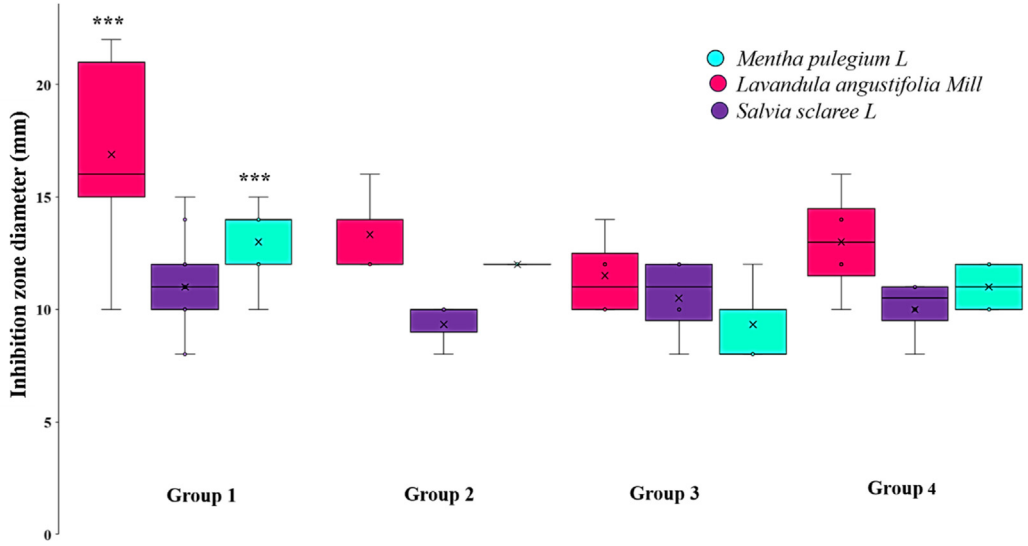

Fig. 5. The antibacterial activity of L. angustifolia Mill, S. sclarea L, and M. pulegium L EOs by disk diffusion correlated with the phenotypic and genotypic characteristics of antibiotic resistance and biofilm formation in S. aureus strains. Error bars indicate standard deviation. Significance was determined using the Kruskal-Wallis test. * $p \leq 0.05$, ** $p \leq 0.01$, *** $p \leq 0.001$.

and imposing stringent limitations on patient care (Kirci et al., 2024). Antibiotic resistance is widely regarded as a major global health issue, contributing to increased illness, death, and financial burden. To address this problem, it is necessary to develop new, potent antimicrobial compounds that reduce dependence on existing antibiotics and the severity of infections.

Given the scarcity of new antibiotics, EOs have emerged as a promising alternative due to their powerful broad-spectrum antibacterial activity, environmental safety, and minimal toxicity to humans. For these reasons, the antimicrobial and anti-biofilm properties of *L. angustifolia* Mill, *S. sclarea* L, and *M. pulegium* L were evaluated against *S. aureus* strains in this study. However, a challenge in using EOs is that the doses required may exceed what consumers are willing to tolerate. To address this issue, we explored the possibility of combining EOs with conventional antibiotics to enhance their efficacy and reduce the required doses.

To our knowledge, this study the first to examine the antimicrobial and anti-biofilm properties of *L. angustifolia* Mill, *S. sclarea* L and *M. pulegium* L EOs, as well as the antimicrobial efficacy of these EOs in combination with antibiotics commonly prescribed to treat *S. aureus* UTIs.

The results of our chemical characterization are not entirely consistent with those of other studies, which report different predominant compounds in the various *Lavandula* oils studied. In the study by El-Akhal et al., the EO of *L. angustifolia* was characterized by a high level of the monoterpene alcohol linalool (32.23%), which was not identified in our sample. Other key compounds included linalyl acetate (14.23%), geraniol (5.8%), lavandulyl acetate (4.8%), and camphor (4.21%), while the 1,8-cineole detected in a high amount in our EO was only present as a minor constituent (2.25%) (El-Akhal et al., 2021). Similarly, in a study of *L. angustifolia* subsp from South Africa, linalool and linalyl acetate were the main compounds, linalool and

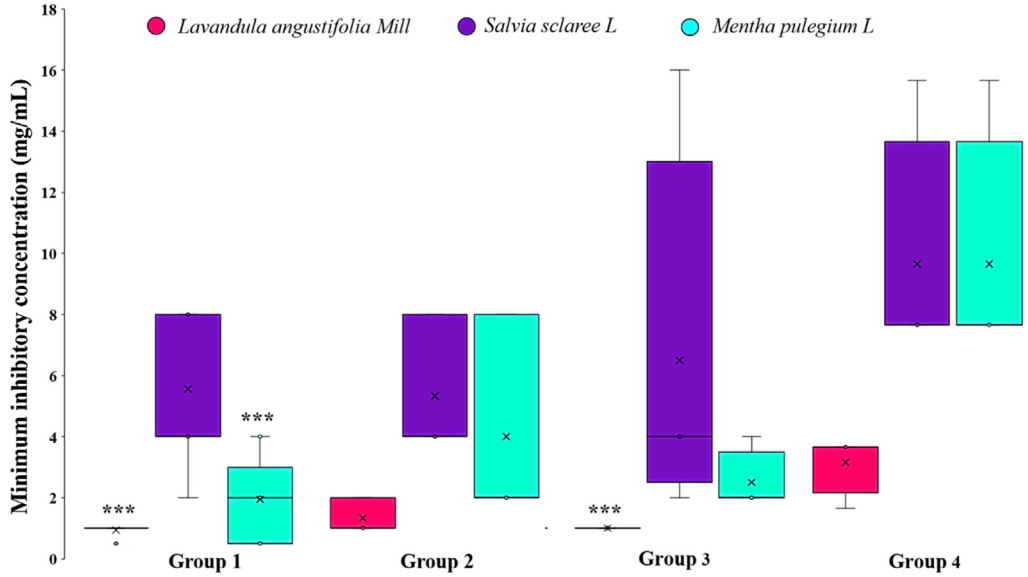

Fig. 6. Correlation between the MICs of EOs of L. angustifolia Mill, S. sclarea L, and M. pulegium L using the Modified Broth Microdilution Method, as well as the phenotypic and genotypic characteristics of antibiotic resistance and biofilm formation against S. aureus strains. Error bars indicate the standard deviation. Significance was determined using Kruskal-Wallis's test. * $p \leq 0.05$, ** $p \leq 0.01$, *** $p \leq 0.001$.

Table 4
Rate of inhibition in biofilm formation (%).

Strain	*L. angustifolia* Mill				*S. sclarea* L				*M. pulegium* L				*Gentamicin*		
	MIC/2	MIC/4	MIC/8	MIC/16	MIC/2	MIC/4	MIC/8	MIC/16	MIC/2	MIC/4	MIC/8	MIC/16	MIC/2	MIC/4	MIC/8
Usa 220321	26.9 ±2.3	21.8 ±1.2	19.1 ±1.8	9.4 ±0.8	22.3 ±3.1	12.6 ±2.3	9.8 ±1.5	4.7 ±0.9	22.3 ±1.8	17.3 ±2.1	14.5 ±1.9	8.5 ±1.5	25.3 ±1.7	10.09 ±2.9	3.80 ±3.1^{S}
Usa 040521	71.1 ±3.1	65.7 ±3.5	59.5 ±3.6	22.3 ±1.2	62.8 ±4.2	61.5 ±4.5	12.2 ±2.1	3.8 ±1.3	67.0 ±4.2	61.6 ±3.9	55.3 ±3.4	26.5 ±3	15.9 ±1.5	10.2 ±1^{S}	17.5 ±1.3^{S}
Usa 080421	60.9 ±2.6	59.8 ±2.9	53.8 ±3.2	33.3 ±2.5	55.5 ±3.5	54.4 ±2.8	48.4 ±1.8	33.2 ±3.1	55.5 ±3.6	54.4 ±4.1	48.5 ±3.6	27.8 ±2	52.1 ±2.1^{S}	65.7±2.5^{S}	84.31±5^{S}
Usa 210321	29.5 ±3.1	25.1 ±2.3	2.4 ±2.1	1.7 ±0.8	22.2 ±1.4	17.9 ±2.1	9.78 ±2.1	3.9± 2.1	22.2 ±3.2	19.3 ±2.8	12.0 ±1.4	3.2±1	6.67 ±1.8^{S}	27.7 ±3.8^{S}	57.7 ±1.5^{S}
Usa 150421	26.4 ±1.5	17.7 ±2.6	14.8 ±1.8	4.2 ±0.9	16.7 ±1.8	8.1 ±1.2	5.16 ±2.2	1.3 ±0.5	16.8 ±1.9	14.8 ±2.4	4.2 ±0.8	2.3 ±0.5	5.57 ±1.1^{S}	27 ±2.8^{S}	34.1 ±3.5^{S}
Usa 210921	48.1 ±1.9	41.9 ±2.8	39.5 ±2.5	7.7 ±1.3	41.9 ±2.3	35.8 ±2.5	31.5 ±2.3	13.8 ±2.1	51.1 ±3.5	45.0 ±2.3	38.3 ±2.6	1.6 ±0.7	94.1 ±5.1	74.2 ±2.8	39.5 ±1.1^{S}
Usa 101121	53.5 ±2.1	55 ±3.7	47.1 ±1.8	34.3 ±2.8	46.4 ±2.1	40.7 ±2.8	32.8 ±1.6	14.2 ±1.7	49.3 ±3.6	42.1 ±3.1	34.3 ±2.1	21.4 ±2	25.9 ±2.9	5.2 ±1.4^{S}	12.5 ±3.3^{S}
Usa 191121	44.7 ±2.4	21.6 ±1.6	38.1 ±3.1	16.4 ±1.2	37.3 ±1.8	17.9 ±1.9	10.4 ±1.3	2.2 ±1.2	39.6 ±3.2	32.8 ±3.2	24.6 ±3.1	9 ±1.5	27.1 ±2.3^{S}	39.3 ±4.1^{S}	57.4 ±5.2^{S}
Usa 161121	51.2 ±2.6	50.5 ±2.7	32.3 ±2.9	12.6 ±0.8	36.6 ±1.1	28.6 ±1.5	25 ±3.2	6.0 ±1.3	43.9 ±3.1	43.2 ±2.5	39.6 ±2.9	19.9 ±1	29.7 ±2.3^{S}	35.03±2.8^{S}	49.28 ±1.9^{S}
Usa 181121	69.2 ±2.7	66.1 ±3.2	62.9 ±3.6	29 ±1.2	51.3 ±1.3	39.3 ±2.8	23.2 ±3.4	11.1 ±1.8	68.3 ±4.1	63.4 ±3.7	59.8 ±2.3	15.6 ±2	32.9 ±2.1	6.2 ±1.9^{S}	22.5 ±3.3^{S}
Usa 271221	44.4 ±3.2	41.4 ±2.8	32.1 ±2.5	28.3 ±2.4	36.7 ±1.3	33.6 ±3.1	24.4 ±2.5	20.5 ±2.4	37.5 ±2.8	32.9 ±2.1	29.0 ±3.1	15.2 ±1	6.72 ±1.5^{S}	21 ±3.2^{S}	-51.7 ±5.8^{S}
Usa 010422	44.5 ±3.9	41.3 ±2.5	32.1 ±2.4	28.3 ±2.7	40.2 ±2.1	20.9 ±2	11.9 ±1.7	8.7 ±1.3	41.5 ±2.4	29.3 ±1.6	18.4 ±2.1	12 ±0.9	7.92 ±1.8	34.38 ±4.1^{S}	42.36±1.5^{S}
Usa 180222	61.7 ±4.1	29.5 ±2.4	27.5 ±1.9	13.8 ±1.8	49.7 ±1.9	25.5 ±2.3	23.4 ±3.1	9.7 ±1.4	58.9 ±3.5	31.9 ±3.1	29.5 ±1.9	11 ±0.8	28.5 ±1.8	8.01 ±0.9	1.50 ±2.8^{S}
Usa 260322	61.7 ±4.2	29.6 ±2.1	27.5 ±2.1	13.8 ±1.6	40.6 ±2	26.4 ±3.1	19.3 ±3.6	10.9 ±2.1	49.0 ±3.8	44.5 ±3.6	34.2 ±2.1	27 ±1.2	77.78 ±5.5	81.60 ±3.9	81.25 ±3.6
Usa 200422	52.4 ±2.4	18.3 ±1.5	13.6 ±1.8	2.9 ±1.8	45.7 ±1.4	13.6 ±1.8	11.6 ±2.1	7.5 ±1.6	43.8 ±3.4	11.6 ±1.2	5.6 ±3.5	4.9 ±2.5	71.10 ±3.5	57.50 ± 4.15	57.1 ±2.51
Usa 060722	57.4 ±3.2	53.1 ±2.3	28.6 ±1.6	18.5 ±1.9	54.1 ±2.3	49.7 ±2.1	15.2 ±1.0	11.8 ±1.5	54.1 ±3.6	49.1 ±4.1	32.6 ±2.3	13.9 ±3	58.16 ±3.5	5.38 ±3.5^{S}	29.26±3.1^{S}
Usa 080722	17.5 ±1.8	11.9 ±1.2	10.9 ±1.8	4.4 ±0.7	25 ±2.3	15.63 ±1.5	1.56 ±2.1	0.6 ±0.6	46.6 ±4.1	24.1 ±2.3	10.9 ±1.9	3.4 ±0.6	5.27 ±2.8^{S}	17.7 ±2.8^{S}	35.7 ±4.5^{S}
Usa 220822	70.8 ±3.6	68.8 ±3	39.6 ±2.3	4.5 ±0.6	67.4 ±1.8	65.4 ±4.5	19.5 ±2.5	7.8 ±0.9	72.8 ±5.6	69.8 ±3.3	49.4 ±2.3	12.5 ±1	4.47 ±1.1^{S}	17 ±3.8^{S}	24.2 ±2.5^{S}
Usa 290822	11.3 ±1.3	17.7 ±2.8	10.4 ±1.5	6.7 ±0.7	28.6 ±2.3	17.68 ±1.2	3.04 ±1.8	1.21 ±1.2	20.4 ±1.9	13.1 ±1.9	14.0 ±2.1	8.5 ±1.2	64.1 ±5.1	54.1 ±2.8	29.5 ±2.1^{S}
Usa 300822	34.2 ±2.3	28.2 ±1.4	18.8 ±1.8	6.8 ±1.3	23.0 ±1.8	11.11 ±1.8	7.69 ±1.4	4.27 ±1.3	42.7 ±3.6	36.8 ±2.3	15.4 ±1.7	6 ±1.3	15.9 ±2.1	3.2 ±1.4^{S}	6.5 ±3.3^{S}
ATCC 43300	40.4 ±3.2	39.4 ±2.5	32.1 ±2.5	25.3 ±2.8	39.7 ±2.3	35.6 ±3.1	25.4 ±1.5	21.5 ±1.4	36.5 ±1.8	29.9 ±1.9	28.0 ±2.1	18.2 ±1.8	17.8 ±2.3^{S}	29.4 ±2.1^{S}	47.4 ±4.2^{S}
ATCC 25923	68.7 ±4.2	30.6 ±2.1	28.5 ±1.6	16.1 ±1.8	43.6 ±1.5	23.6 ±2	20.3 ±2.6	11.6 ±1.1	48.0 ±2.3	45.1 ±3.6	33.2 ±1.1	21 ±3.2	39.7 ±2.3	25.03±2.8	19.28 ±1.9

S: Increased biofilm formation; MIC: Minimum inhibitory concentration.

linalyl acetate were the major components, with linalyl acetate contributing 36.7% and linalool 31.4%. (de Rapper et al., 2016), Notably, both linalool and linalyl acetate are typical constituents of lavender EOs and are often among the top ten major components in the EOs of fresh flowers of many Ukrainian *L. angustifolia* cultivars, where camphor and 1,8−cineole are absent (Pokajewicz et al., 2021). This finding is contrasts with that of Nurzyńska et al., who found that the EO of *Lavandula angustifolia* Mill extracted from leaves was rich in epi-α-cadinol (17.8%), cryptone (10.4%), 1,8−cineole (7.3%), and caryophyllene oxide (7.2%), while the EO obtained from flowers was dominated by linalyl acetate (32.1%) and linalool (29.9%) (Nurzynska-Wierdak and Zawislak, 2016).

Regarding the chemical composition of *S. sclarea* L, our results align with those reported by Kacániová et al., who identified 99.6% of the bioactive compounds in the EO of *S. sclarea* grown in Slovakia. The majority of the compound belonged to the oxygenated monoterpene class (82.4%), with linalyl acetate (49.1%) and linalool (20.6%) being the most abundant (Kačániová et al., 2023). Generally, the EO of *S. sclarea* L contains numerous compounds from different classes, including monoterpene esters (linalyl acetate and neryl acetate), monoterpene alcohols (linalool and α-terpineol), sesquiterpene hydrocarbons (germacrene-D, α-humulene, and caryophyllene), and oxygenated sesquiterpenes (caryophyllene oxide)(Hans et al., 2023).

The pulegone has been also been identified as the main compound in the volatile profile of Moroccan pennyroyal EO (74.03%), with carvone (5.45%) and dihydrocarvone (3.66%) present in lower amount (Ramzi et al., 2022). Conversely, the EO of another species of *M. pulegium* L was dominated by piperitenone (32.9%) and pulegone (32.8%) (Gourich et al., 2022). It is worth noting that the pennyroyal EO typically belongs to the “pulegone” chemotype (>70%), as commonly reported in the literature (Aimad et al., 2021; Messaoudi et al., 2022). However, the EO extracted from Tunisian *M. pulegium* exhibited a significant variation in its chemical profile, with a higher abundance of esters and alcohol such as 1,8−cineole (14,60%) and menthol (8,76%), as well as the ketones like p-menthan-3-one (14,9%), and piperitenone (11,4%) (Chaaban et al., 2019). A more recent study by Yakhlef et al. also found a high level of sesquiterpene (36.03%) in the EO of *M. pulegium* from Algeria, with piperitenone oxide (35.49) and caryophyllene oxide (35.27) as the major constituents (Yakhlef et al., 2020).

Several factors can influence the quantitative and the qualitative composition of EOs, including geographical location, climatic

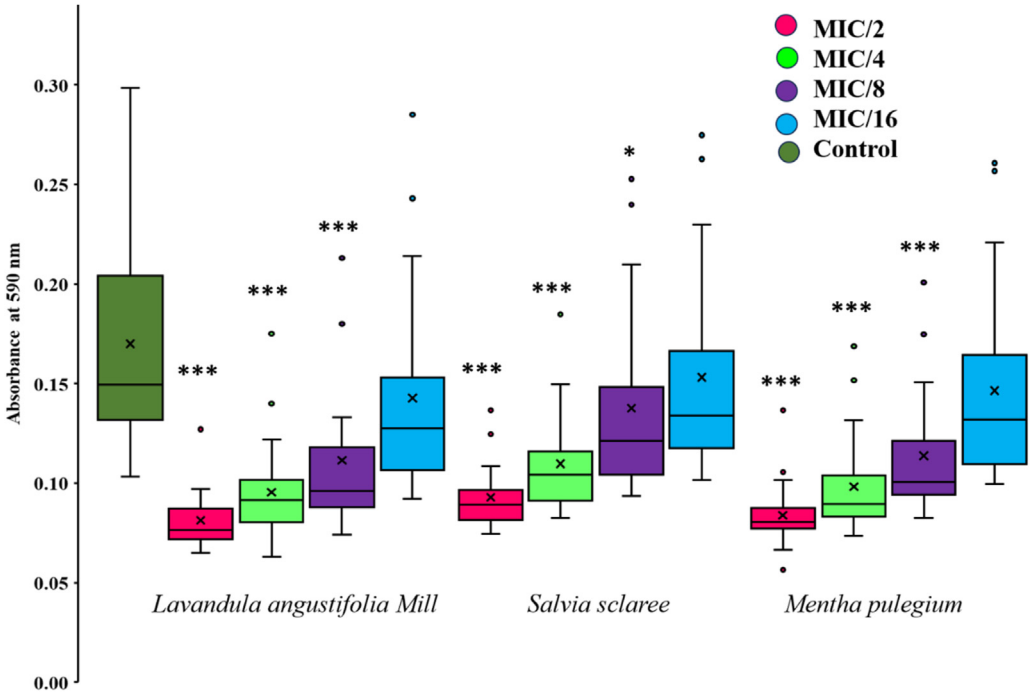

Fig. 7. Inhibition of biofilm formation by sub-MIC of L. angustifolia Mill, S. sclarea L, and M. pulegium L EOs for S. aureus isolates, with results reported in comparison with the control for that isolate in the absence of EOs. Error bars indicate standard deviation. Significance was determined using Dunnett's test. * $p \leq 0.05$, ** $p \leq 0.01$, *** $p \leq 0.001$.

conditions (temperature, relative humidity, sunlight, air movement and precipitation during plant development), as well as agronomic factors such as fertilization and irrigation (Li et al., 2020).

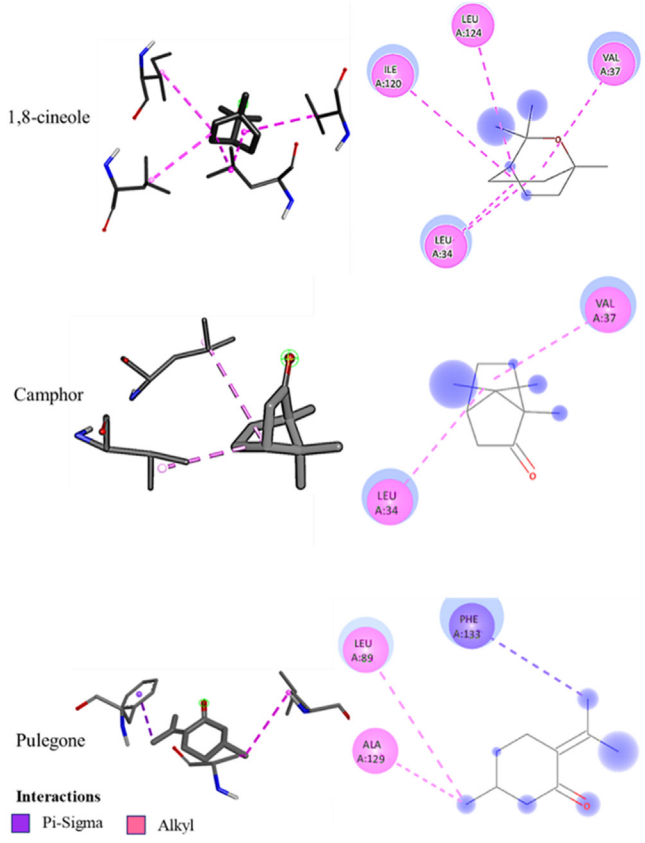

Fig. 8. 2D and 3D interactions of major chemical compounds extracted from L. angustifolia Mill, S. sclarea L, and M. pulegium L EOs with PLP2a protein receptors.

These EOs showed antibacterial activity against all of the tested *S. aureus* strains. Interestingly, the *L. angustifolia* Mill and *M. pulegium* L EOs showed significant antibacterial efficacy against MSSA compared with MRSA. These differences may be explained by variations in the rate at which the EOs constituents penetrate the cell wall and membrane structures.

The antibacterial properties of EOs are generally attributed to their chemical composition. The mechanism of action of each compound may vary depending on the biochemical reactions that occur in bacterial cells and the type of bacteria targeted (Badr et al., 2021). The antimicrobial properties of the *M. pulegium* L EO are attributed to their pulegone, menthone, and neomenthone components, which cause bacterial lysis by altering cell membrane permeability and disrupting the structure of various polysaccharides, fatty acids, and phospholipids in the bacterial cell membrane (Oualdi et al., 2023). Furthermore, we suggest that the antibacterial and antibiofilm activities of the *L. angustifolia* Mill are associated with high concentrations of 1,8-cineole. The broad-spectrum antimicrobial potency of these oxygenated monoterpenes has been well documented in previous studies and reviews (Blažeković et al., 2018). The structural properties of 1,8-cineole enable it to disrupt bacterial membrane integrity and membrane-associated functions such as permeability, membrane transport, energy production, and cell signaling (Blažeković et al., 2018). In addition, 1,8−cineole inhibits biofilm formation and quorum sensing, making it a promising candidate for the development of new and effective antibacterial and antibiofilm agents (Blažeković et al., 2018). However, it is clear that this antimicrobial activity cannot be attributed only to the major compound (1,8-cineole), because an EO is a complex mixture of many volatile constituents. Other minor compounds present in the studied EOs, such as ketones and naphthalenes, could contribute to this activity (Magaji et al., 2023).

The antimicrobial activity of the *S. Sclerae* L EOs could be attributed to the high concentration of linalyl acetate. This finding is in line with previous reports revealing that this acyclic monoterpenoid plays a crucial role in the antibacterial activity of the *S. Sclerae* EO against *S. aureus* strains (Aćimović et al., 2022; Kwiatkowski et al., 2020).

Table 5
Correlation between the rate of inhibition of biofilm formation by *L. angustifolia Mill, S. sclarea,* and *M. pulegium* EOs and phenotypic and genotypic characteristics of antibiotic resistance and biofilm formation by *S. aureus* strains.

Essential oils	Sub-MIC	Group 1	Group 2	Group 3	Group 4	*P value*
L. angustifolia Mill	MIC/2	51.77±14.6	56.27±9.6	45.28±9.63	30.4±16	0.756
	MIC/4	41.44±16.9	55.03±9.1	33.65±13.6	23.28±9.31	0.715
	MIC/8	33.28±16.9	39.60±5	23.35±7	24.73±14.1	0.943
	MIC/16	15.28±8.61	22.37±11.9	14.78±8.63	8.8±3.8	0.955
S. sclarea L	MIC/2	39.82±13.5	51.33±10.7	39.7±10.2	33.2±6.40	0.989
	MIC/4	30.31±14.2	42.33±15.3	27.38±14.2	21.7±7.02	0.315
	MIC/8	19.35±9.47	21.4±7.6	15.25±4.58	11.63±9.94	0.631
	MIC/16	9.35±6.11	10.23±2.6	11.13±5.03	4.45±4.67	0.732
M. pulegium L	MIC/2	47.14±14.0	54.53±12.1	39.43±9.53	39.43±9.51	0.693
	MIC/4	41.1±13.6	47.07±15.1	27.73±13.2	28.75±10.2	0.913
	MIC/8	33.17±15.9	34.03±10.4	20.43±10.4	21.95±9.5	0.994
	MIC/16	15.48±8.76	15.3±4.07	10.58±3.88	5.63±3.13	0.332

MIC: Minimum inhibitory concentration

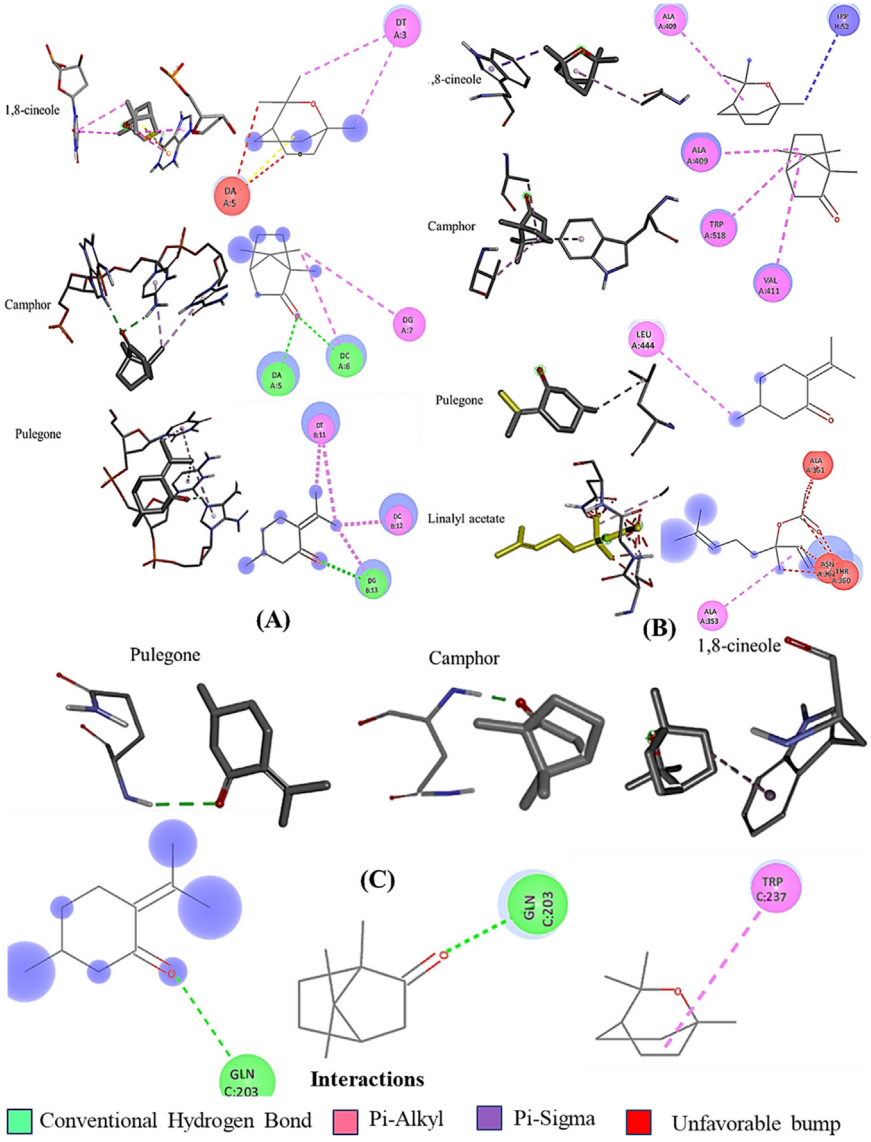

Fig. 9. 2D and 3D interactions of major chemical compounds extracted from L. angustifolia Mill L, S. sclarea L, and M. pulegium L EOs with Bap (A), ClfA (B), and FnbB (C) protein receptors.

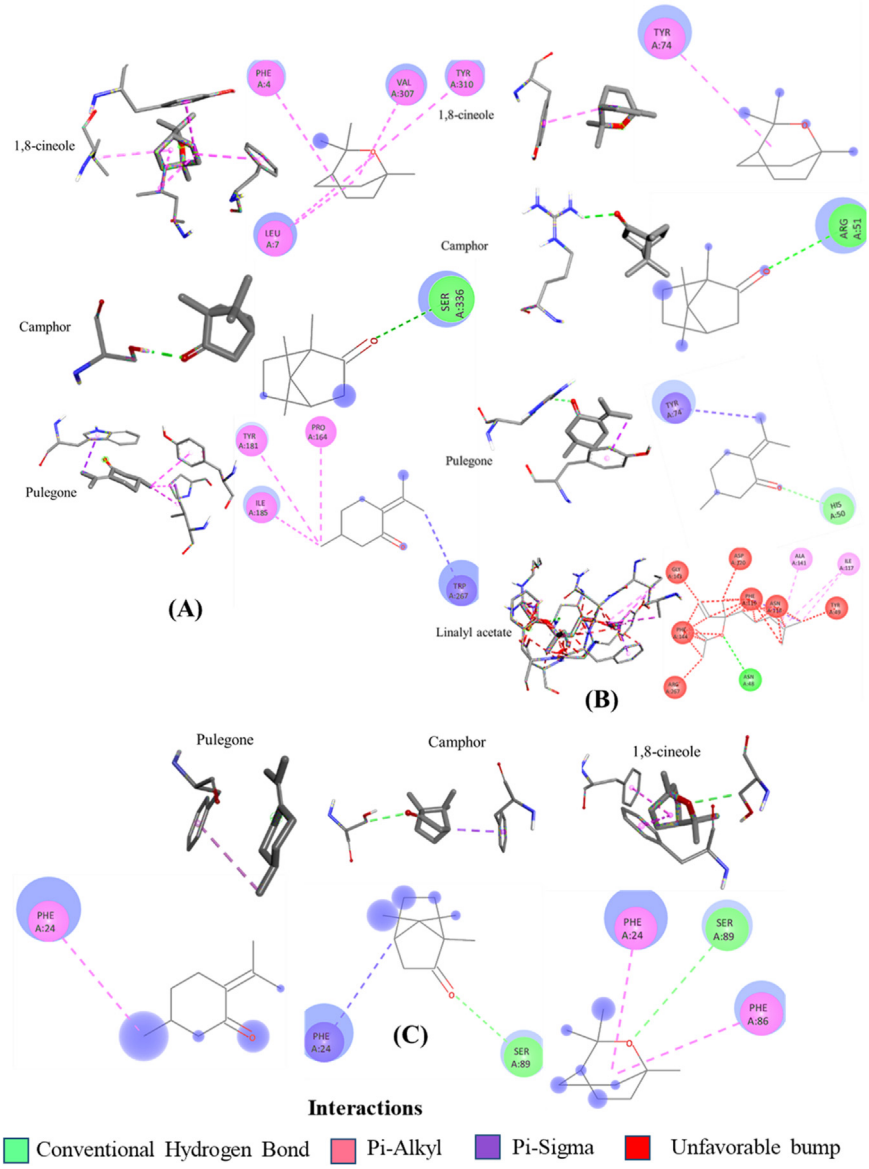

Fig. 10. 2D and 3D interactions of major chemical compounds extracted from L. angustifolia Mill, S. sclarea L, and M. pulegium L EOs with IcaA (A), IcaB (B), and IcaD (C) protein receptors.

We observed synergistic interactions between the *L. angustifolia* Mill, *S. sclarea* L, and *M. pulegium* L EOs, and conventional antibiotic agents used to treat *S. aureus* UTIs. The combination of the *L. angustifolia* Mill EO and gentamicin showed the greatest synergistic antibacterial effects against MSSA and MRSA. Some studies have also suggested that this result may be due to the positive interactions between the main constituents of EOs, in particular, oxygenated monoterpenes, and antibiotics (Adaszyńska-Skwirzyńska et al., 2023).

Combination of the *M. pulegium* L EO with levofloxacin and vancomycin showed significant synergistic effects against both MSSA and MRSA. Some studies have emphasized the significant synergistic effects of *M. pulegium* L EO when used in combination with various classes of antibiotics, including penicillin, cephalosporins, carbapenems, and aminoglycosides, against MDR bacteria (Bekka-Hadji et al., 2022). In general, many mechanisms can lead to pharmacological synergy between EOs and antibiotics, including multi-target effects, in which compounds target different sites in the bacterial cell; pharmacokinetic or physicochemical effects (improved solubility or bioavailability); and targeting of a specific bacterial resistance mechanism (Langeveld et al., 2014).

The persistence of MDR-*S. aureus* cells in biofilm is a significant factor in the global burden of severe infections. Biofilms, which form on both biotic and abiotic surfaces, pose a serious public health challenges, including antibiotic resistance and chronic infections. Consequently, there is an urgent need for novel strategies to either eliminate preformed biofilms or to prevent biofilm formation altogether, particularly through the use of natural, alternative antimicrobial agents. These alternative strategies represent innovative and promising solutions for biofilm management.

In the current study, the *L. angustifolia* Mill, *S. sclarea* L, and *M. pulegium* L EOs showed significant antibiofilm activity against *S. aureus* strains across a range of concentrations (MIC, MIC/2, MIC/4, MIC/8 and MIC/16). We observed the most notable reductions in biofilm were observed at MIC/2, MIC/4, and MIC/8, compared with untreated *S. aureus*. These results can be attributed to the inhibition of gene expression that essential for the synthesis of proteins and lipopolysaccharides in the bacterial outer membrane. These genes are

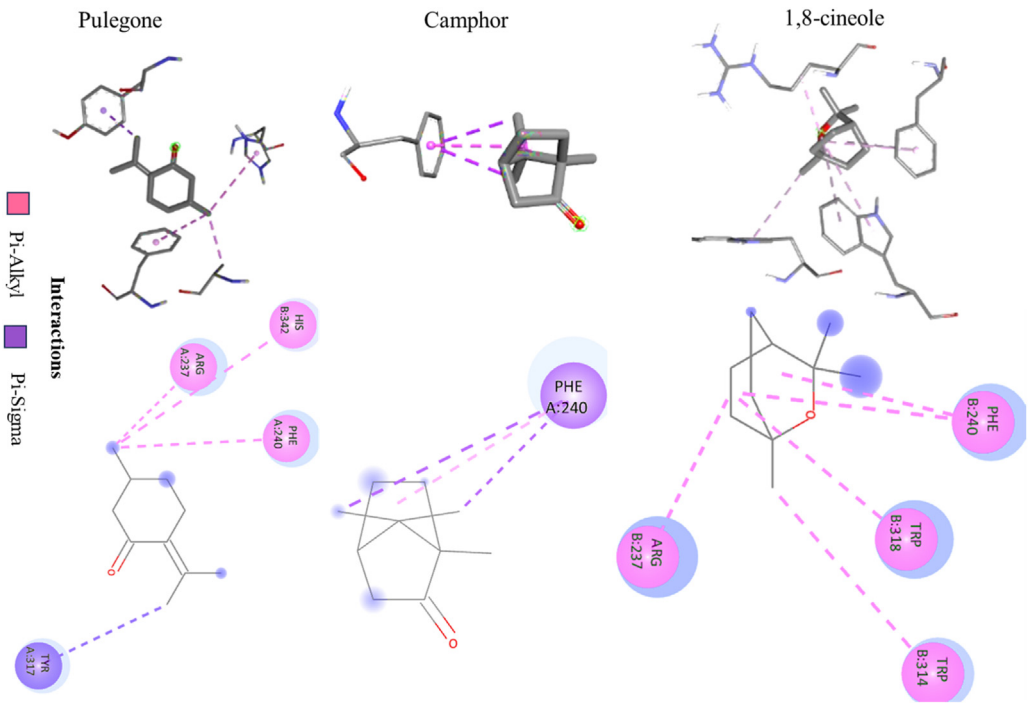

Fig. 11. 2D and 3D interactions of major chemical compounds extracted from *L. angustifolia* Mill, *S. sclarea* L, and *M. pulegium* L EOs with Poly-β (1,6)-N-acetyl-D-glucosamine protein receptors.

critical for the initial adhesion of bacterial cells to both abiotic and biotic surfaces and for the subsequent development of biofilm structure.

Moreover, the components of these EOs appear to play a role in regulating of the expression of flagellar genes, genes associated with nutrient absorption systems, and stress defense and motility genes. This suggests that exposure to these EOs induces significant stress in *S. aureus* strains, potentially disrupting key cellular processes required for biofilm formation.

Comprehensive transcriptomic analysis can offer new insights into potential molecular targets for combating antibiotic resistance and biofilm formation, providing promising avenues for further research in fight against this pathogenic bacterium.

In addition, biofilms are notoriously difficult to eliminate with standard antibiotic treatments due to their heightened resistance to these agents compared to planktonic cells (Rosato et al., 2020). In this study, we demonstrated that antimicrobial EOs can more effectively eradicate bacteria in biofilms than some commonly used antibiotics, making them promising candidates for biofilm treatment.

The compounds primarily found in *L. angustifolia* Mill, *S. sclarea* L, and *M. pulegium* L EOs, including 1,8-cineole, camphor, linalyl acetate, and pulegone, were analyzed by molecular docking to determine their probable mode of action and binding efficiency with various receptors.

Docking analysis revealed that the interaction of 1,8−cineole and camphor with the intercellular adhesion active site residues, responsible for the synthesis of intercellular polysaccharide adhesin (IPA), including IcaA, IcaB, and IcaD, as well as bacterial adhesion proteins (Bap, FnbB, and ClfA), and exopolysaccharide biofilm-associated molecule (PNAG), were mediated by hydrophobic interactions and hydrogen bonds. These hydrogen bonds strengthen and stabilize the bonds between the target and the ligand, thereby contributing to the potent antibacterial and antibiofilm activities of *L. angustifolia* Mill EO (Sharma and Kaur, 2022). Furthermore, the antibacterial and antifilm activity of *M. pulegium* L against *S. aureus* is attributed to the intermolecular interactions, such as pi-sigma and pi-alkyl bonds, detected between pulegone and the PLP2a, Bap, ClfA, IcaA, IcaB, IcaD and PNAG proteins.

The major constituents of *L. angustifolia* Mill, *S. sclarea* L, and *M. pulegium* L EOs are non-toxic, well-absorbed, and have excellent ADME profiles, which makes the promising candidates for further investigation in therapeutic contexts.

While this study provides valuable insights into the antimicrobial and anti-biofilm activities of these EOs, certain limitations need to be addressed in future research. Expanding the scope of research to include more comprehensive, multi-faceted approaches could provide a deeper understanding of their therapeutic potential and facilitate their clinical applications. It should be noted that this study was conducted *in vitro*, which does not account for the complexity of *in vivo* conditions, including the immune system, pharmacokinetics, and tissue penetration. Therefore, future studies should evaluate the efficacy of these EOs in animal models to confirm their potential therapeutic effects under realistic biological conditions.

Additionally, the composition of EOs can vary based on factors such as the plant source, harvest time, and extraction method. This variability may influence the reproducibility of results. Standardizing of the extraction procedures and providing detailed chemical profiles of the EOs would enhance the reliability and comparability of the findings across studies. Furthermore, while *in silico* molecular docking studies provide valuable insights, they do not always capture the full complexity of biological interactions. It is recommended that these studies be to molecular dynamics simulations and that predictions be validated through laboratory experiments. such approaches will strengthen the evidence supporting the mechanism of action of EOs and improve their potential for therapeutic use.

Table 6
ADMET properties of bioactive compounds used as ligands.

ADME	Ligand			
	1,8-cineole	**Camphor**	**Linalyl acetate**	**Pulegone**
Physicochemical Properties				
Formula	$C_{10}H_{18}O$	$C_{10}H_{16}O$	$C_{10}H_{18}O$	$C_{10}H_{16}O$
Molecular weight	154,25 g/mol	152,23 g/mol	196,29 g/mol	153,23 g/mol
Num. heavy atoms	11	11	14	12
Num. arom. heavy atoms	0	0	0	0
Fraction Csp3	1.00	0.90	0.58	0.73
Num. rotatable bonds	0	0	6	0
Num. H-bond acceptors	1	1	2	1
Num. H-bond donors	0	0	0	0
Molar Refractivity	47.12	45.64	60.17	52.60
TPSA	9.23 $Å^2$	17.07 $Å^2$	26.30 $Å^2$	17.07 $Å^2$
Lipophilicity				
Log *Po/w* (iLOGP)	2.58	2.12	3.08	2.53
Log *Po/w* (XLOGP3)	2.74	2.19	3.93	3.37
Log *Po/w* (WLOGP)	2.74	2.40	3.24	2.96
Log *Po/w* (MLOGP)	2.45	2.30	2.95	2.49
Log *Po/w* (SILICOS-IT)	2.86	2.85	2.98	2.84
Consensus Log *Po/w*	2.67	2.37	3.24	2.84
Water Solubility				
Log S (ESOL)	-2.52	-2.16	-3.14	-2.99
Solubility	4.63×10^{-1} mg/mL; 3×10^{-3} mol/L	1.04 mg/mL; 6×10^{-3} mol/L	1.43×10^{-1} mg/mL; 7.30×10^{-4}mol/L	1.69×10^{-1}mg/mL; 1.01×10^{-3}mol/L
Class	Poorly Soluble	Moderately Soluble	Poorly Soluble	Moderately Soluble
Log S (Ali)	-2.59	-2.18	-4.18	-3.41
Solubility	3.98×10^{-1} mg/mL; 2.58×10^{-3} mol/L	1mg/mL; 6.57×10^{-3} mol/L	1.29×10^{-2} mg/mL; 6.58×10^{-5} mol/L	6.52×10^{-2} mg/mL; 3.92×10^{-4} mol/L
Class	Soluble	Soluble	Moderately soluble	Soluble
Log S (SILICOS-IT)	-2.45	-2.60	-2.52	-2.55
Solubility	5.45×10^{-1} mg/mL; 3.53×10^{-3} mol/L	3.83×10^{-1} mg/mL; 2.52×10^{-3} mol/L	5.97×10^{-1} mg/mL; 3.04×10^{-3} mol/L	4.73×10^{-1} mg/mL; 2.84×10^{-3} mol/L
Pharmacokinetics				
Gastrointestinal absorption	High	High	High	High
Blood-brain barrier permeant	Yes	Yes	Yes	Yes
Permeability-glycoprotein	No	No	No	No
CYP1A2 inhibitor	No	No	No	No
CYP2C19 inhibitor	No	No	No	No
CYP2C9 inhibitor	No	No	No	No
CYP2D6 inhibitor	No	No	No	No
CYP3A4 inhibitor	No	No	No	No
Log Kp (Skin permeation)	-5.30 cm/s	-5.67 cm/s	-4.71 cm/s	-4.92 cm/s
Drug likeness				
Lipinski	Yes; 0 violation	Yes; 0 violation	Yes; 0 violation	Yes; 0 violation
Ghose	No	No	Yes	Yes
Veber	Yes	Yes	Yes	Yes
Egan	Yes	Yes	Yes	Yes
Muegge	No; 2 violations	No; 2 violations	No; 1 violation	No; 2 violations
Bioavailability	0,55	0,55	0,55	0,55
Medicinal Chemistry				
PAINS	0 alert	0 alert	0 alert	0 alert
Brenk	0 alert	0 alert	1 alert: isolated_alkene	1 alert: michael_acceptor_1
Leadlikeness	No; 1 violation	No; 1 violation	No; 2 violations	No; 1 violation
Synthetic accessibility	3.65	3.22	2.75	3.12
Phonic absorption	High	High	High	High

TPSA: Topological polar surface area; log P: Partition coefficient.

Table 7
Toxicity estimation performed by the ProToxll 3.0 package.

Ligand	**1,8-cineole**	**Camphor**	Linalyl acetate	**Pulegone**
Predicted toxicity class	V	IV	VI	IV
Predicted LD50 (mg/kg)	2480	775	12000	470

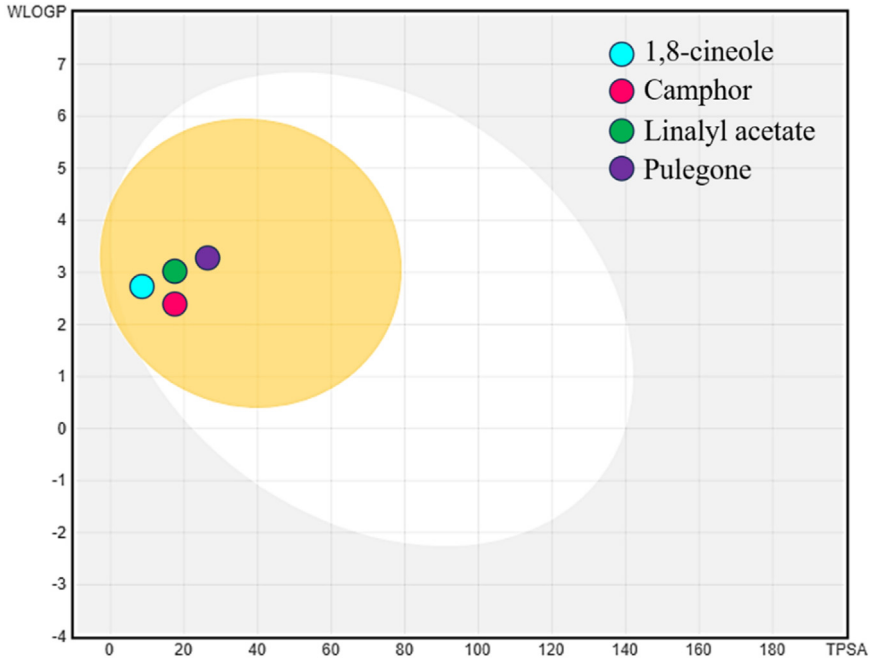

Fig. 12. The predictive Egan Boild-Egg model of four chemical compounds extracted from *L. angustifolia* Mill, *S. sclarea* L, and *M. pulegium* L EOs.

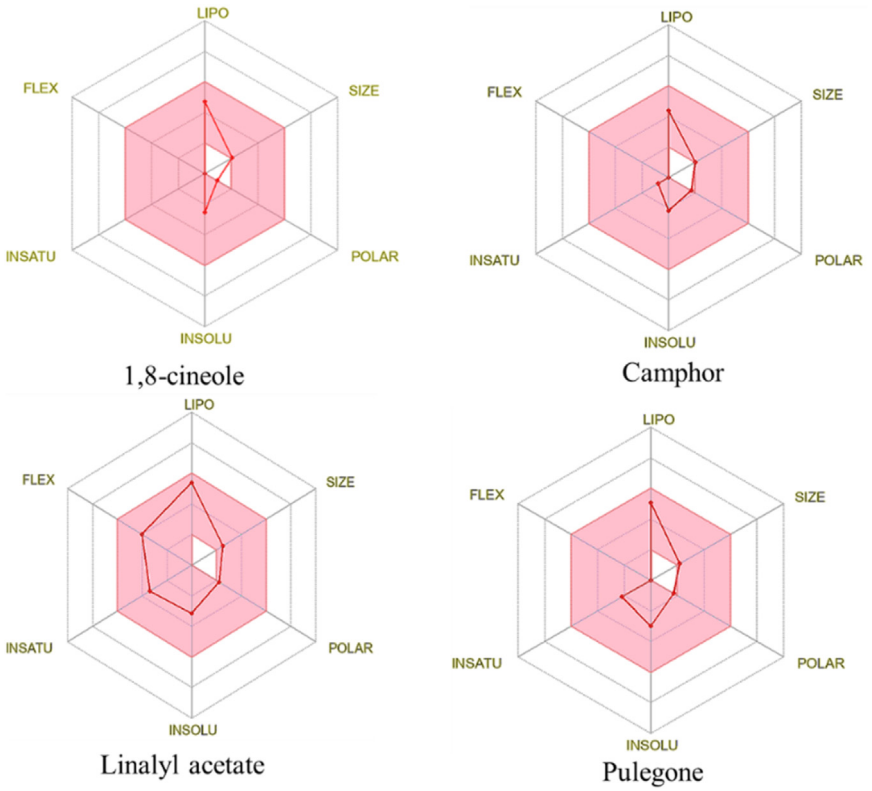

Fig. 13. A radar plot of four chemical compounds extracted from *L. angustifolia* Mill, *S. sclarea* L, and *M. pulegium* L EOs. POLAR (polarity), LIPO (lipophilicity), INSOLU (solubility), FLEX (flexibility), and IN-SATU (saturation).

5. Conclusion

In this study, we evaluated the chemical composition, and antimicrobial and antibiofilm characteristics of the of *L. angustifolia* Mill, *S. sclarea* L, and *M. pulegium* L EOs *in vitro* and *in silico*. We used hydrodistillation to extract the EOs. GC/MS analysis of the EOs showed high levels of various bioactive compounds, mainly 1,8-cineole (*L. angustifolia* Mill), linalyl acetate (*S. sclarea* L), and pulegone (*M. pulegium* L), which are the main contributors to the antibacterial and antibiofilm activities of these EOs. Additionally, various combinations of conventional antibiotics and EOs showed promising synergistic interactions with MSSA and MRSA strains. Our finding indicate that these EOs

merit further exploration for their potential applications in combination with antibiotic therapy to reduce the minimum effective dose of drugs and combat the emergence of drug-resistant bacteria.

Ethical approval

This study was approved by the internal ethics committee of the Biological Geology Department of the polydisciplinary faculty of Sultan Moulay Slimane University, Beni Mellal, and by the Ethics Committee for Biomedical Research of the Faculty of Medicine and Pharmacy of Mohammed I University, Oujda, Morocco, approval number: 15/2023.

Availability of supporting data

The datasets used and analyzed during the current study are available from the corresponding author on reasonable request.

Declaration of competing interest

The authors declare that they have no known competing financial interests or personal relationships that could have appeared to influence the work reported in this paper.

CRediT authorship contribution statement

Rafik Aniba: Conceptualization, Methodology, Software, Formal analysis, Investigation, Resources, Data curation, Writing – original draft. **Amal Ramzi:** Resources, Methodology, Investigation. **Asmaa Dihmane:** Methodology, Investigation, Formal analysis. **Habiba Raqraq:** Software, Investigation. **Amina Ressmi:** Methodology, Investigation, Conceptualization. **Kaotar Nayme:** Visualization, Validation, Supervision. **Mohammed Timinouni:** Writing – review & editing, Validation, Supervision. **El idrissi Mohammed:** Validation, Software, Resources. **Farah Abdellah:** Validation, Supervision. **Abouddihaj Barguigua:** Writing – review & editing, Visualization, Validation, Supervision, Resources, Project administration, Conceptualization.

Funding

No funding

Supplementary materials

Supplementary material associated with this article can be found in the online version at doi:10.1016/j.sajb.2025.03.038.

References

Abers, M., Schroeder, S., Goelz, L., Sulser, A., Rose, St, T., Puchalski, K., Langland, J., 2021. Antimicrobial activity of the volatile substances from essential oils. BMC. Complement. Med. Ther. 21, 124. https://doi.org/10.1186/s12906-021-03285-3.

Aćimović, M.G., Cvetković, M.T., Jeremić, J.M.S., Pezo, L.L., Varga, A.O., Čabarkapa, I.S., Kiprovski, B., 2022. Biological activity and profiling of salvia sclarea essential oil obtained by steam and hydrodistillation extraction methods via chemometrics tools. Flavour. Fragr. J. 37, 20–32.

Adams, R.P., 2017. Identification of Essential Oil Components by Gas Chromatography/Mass Spectrometry, 4th ed. Allured Publishing Corporation: Carol Stream, IL, USA. 2007. Allured Publishing.

Adaszyńska-Skwirzyńska, M., Zych, S., Bucław, M., Majewska, D., Dzięcioł, M., Szczerbińska, D., 2023. Evaluation of the antibacterial activity of gentamicin in combination with essential oils isolated from different cultivars and morphological parts of lavender (Lavandula angustifolia Mill.) against selected bacterial strains. Molecules. 28, 5781. https://doi.org/10.3390/molecules28155781.

Águila-Arcos, S., Álvarez-Rodríguez, I., Garaiyurrebaso, O., Garbisu, C., Grohmann, E., Alkorta, I., 2017. Biofilm-forming clinical Staphylococcus isolates harbor horizontal transfer and antibiotic resistance genes. Front. Microbiol. 8.

Aimad, A., Sanae, R., Anas, F., Abdelfattah, E.M., Bourhia, M., Mohammad Salamatullah, A., Alzahrani, A., Alyahya, H.K., Albadr, N.A., Abdelkrim, A., El Barnossi, A., Noureddine, E., 2021. Chemical characterization and antioxidant, antimicrobial, and insecticidal properties of essential oil from Mentha pulegium L. Evid. Based. Complement. Alternat. Med., 1108133. https://doi.org/10.1155/2021/1108133 2021.

Aniba, R., Dihmane, A., Raqraq, H., Ressmi, A., Nayme, K., Timinouni, M., Hicham, B., Khalil, A., Barguigua, A., 2024. Characterization of biofilm formation in uropathogenic Staphylococcus aureus and their association with antibiotic resistance. The Microbe 2, 100029. https://doi.org/10.1016/j.microb.2023.100029.

Badr, M.M., Badawy, M.E.I., Taktak, N.E.M., 2021. Characterization, antimicrobial activity, and antioxidant activity of the nanoemulsions of Lavandula spica essential oil and its main monoterpenes. J. Drug Deliv. Sci. Technol. 65, 102732. https://doi.org/10.1016/j.jddst.2021.102732.

Bekka-Hadji, F., Bombarda, I., Djoudi, F., Bakour, S., Touati, A., 2022. Chemical composition and synergistic potential of Mentha pulegium L. and Artemisia herba alba asso. Essential oils and antibiotic against multi-drug resistant bacteria. Molecules. 27, 1095. https://doi.org/10.3390/molecules27031095.

Blažeković, B., Yang, W., Wang, Y., Li, C., Kindl, M., Pepeljnjak, S., Vladimir-Knežević, S., 2018. Chemical composition, antimicrobial and antioxidant activities of essential oils of lavandula × intermedia 'Budrovka' and L. angustifolia cultivated in Croatia. Ind. Crops. Prod. 123, 173–182. https://doi.org/10.1016/j.indcrop.2018.06.041.

Bolouri, P., Salami, R., Kouhi, S., Kordi, M., Asgari Lajayer, B., Hadian, J., Astatkie, T., 2022. Applications of essential oils and plant extracts in different industries. Molecules. 27, 8999. https://doi.org/10.3390/molecules27248999.

Chaaban, S.B., Hamdi, S.H., Mahjoubi, K., Jemàa, J.M.B., 2019. Composition and insecticidal activity of essential oil from Ruta graveolens, Mentha pulegium and Ocimum basilicum against Ectomyelois ceratoniae Zeller and Ephestia kuehniella Zeller (Lepidoptera: Pyralidae). J. Plant Dis. Protect. 126, 237–246.

CLSI, I., 2018. Performance Standards for Antimicrobial Disk and Dilution Susceptibility Tests for Bacteria Isolated from Animals. CLSI supplement VET08.

Council of Europe, European Pharmacopoeia Commission, 2007. European Pharmacopoeia, 6th ed. Council Of Europe, Strasbourg.

Cutro, A.C., Coria, M.S., Bordon, A., Rodriguez, S.A., Hollmann, A., 2023. Antimicrobial properties of the essential oil of Schinus areira (Aguaribay) against planktonic cells and biofilms of S. aureus. Arch. Biochem. Biophys. 744, 109670. https://doi.org/10.1016/j.abb.2023.109670.

de Rapper, S., Viljoen, A., van Vuuren, S., 2016. The *In vitro* antimicrobial effects of *lavandula angustifolia* essential oil in combination with conventional antimicrobial agents. Evidence-Based Compl. Alternat. Med., e2752739. https://doi.org/10.1155/2016/2752739 2016.

Didier, D., 2000. Huiles essentielles. (3 Vol.) Tome 2 Volume 1 : Monographies relatives aux huiles essentielles (A à G)., Recueil normes. Association française de normalisation (AFNOR), Paris - La Défense.

El-Akhal, F., Ramzi, A., Farah, A., Ez Zoubi, Y., Benboubker, M., Taghzouti, K., El Ouali Lalami, A., 2021. Chemical composition and larvicidal activity of *Lavandula angustifolia* subsp. *Angustifolia* and *Lavandula dentata* spp. *Dentata* essential oils against *culex pipiens* larvae, vector of West Nile Virus. Psyche: J. Entomol., e8872139. https://doi.org/10.1155/2021/8872139 2021.

Elshikh, M., Ahmed, S., Funston, S., Dunlop, P., McGaw, M., Marchant, R., Banat, I.M., 2016. Resazurin-based 96-well plate microdilution method for the determination of minimum inhibitory concentration of biosurfactants. Biotechnol. Lett. 38, 1015–1019. https://doi.org/10.1007/s10529-016-2079-2.

Gourich, A.A., Bencheikh, N., Bouhrim, M., Regragui, M., Rhafouri, R., Drioiche, A., Asbabou, A., Remok, F., Mouradi, A., Addi, M., Hano, C., Zair, T., 2022. Comparative analysis of the chemical composition and antimicrobial activity of four Moroccan North Middle Atlas medicinal plants' Essential oils: Rosmarinus officinalis L., Mentha pulegium L., salvia officinalis L., and Thymus zygis subsp. gracilis (Boiss.) R. Morales. Chem. 4, 1775–1788. https://doi.org/10.3390/chemistry4040115.

Hans, M., Deeksha Nayik, G.A., Salaria, A., 2023. Chapter 19 - clary sage essential oil, in: Nayik, G.A., Ansari, M.J. (Eds.), Essential Oils. Academic Press, pp. 459–478. https://doi.org/10.1016/B978-0-323-91740-7.00001-3

Hashemzadeh, M., Dezfuli, A.A.Z., Nashibi, R., Jahangirimehr, F., Akbarian, Z.A., 2021. Study of biofilm formation, structure and antibiotic resistance in Staphylococcus saprophyticus strains causing urinary tract infection in women in Ahvaz, Iran. New Microbes New Infect. 39, 100831. https://doi.org/10.1016/j.nmni.2020.100831.

Iseppi, R., Cerbo, A.D., Aloisi, P., Manelli, M., Pellesi, V., Provenzano, C., Camellini, S., Messi, P., Sabia, C., 2020. In vitro activity of essential oils against planktonic and biofilm cells of extended-spectrum β-lactamase (ESBL)/carbapenamase-producing gram-negative bacteria involved in Human nosocomial infections. Antibiotics 9. https://doi.org/10.3390/antibiotics9050272.

Jaber, H., Oubihi, A., Ouryemchi, I., Boulamtat, R., Oubayoucef, A., Bourkhiss, B., Ouhssine, M., 2021. Chemical composition and antibacterial activities of eight plant essential oils from Morocco against Escherichia coli strains isolated from different Turkey organs. Biochem. Res. Int., 6685800. https://doi.org/10.1155/2021/6685800 2021.

Kačániová, M., Vukovic, N.L., Čmiková, N., Galovičová, L., Schwarzová, M., Šimora, V., Kowalczewski, P.Ł., Kluz, M.I., Puchalski, C., Bakay, L., Vukic, M.D., 2023. Salvia sclarea essential oil chemical composition and biological activities. Int. J. Mol. Sci. 24, 5179. https://doi.org/10.3390/ijms24065179.

Kirci, D., Batur, Ö.Ö., Demirci, B., 2024. Antimicrobial combination of Lavandula Angustifolia L. ESSENTIAL oil with Kojic Acid. J. Fac. Pharm. Ankara 48, 197–204. https://doi.org/10.33483/jfpau.1399176.

Kwiatkowski, P., Łopusiewicz, Ł., Pruss, A., Kostek, M., Sienkiewicz, M., Bonikowski, R., Wojciechowska-Koszko, I., Dołęgowska, B., 2020. Antibacterial activity of selected essential oil compounds alone and in combination with β-lactam antibiotics against MRSA strains. Int. J. Mol. Sci. 21, 7106. https://doi.org/10.3390/ijms21197106.

Langeveld, W.T., Veldhuizen, E.J.A., Burt, S.A., 2014. Synergy between essential oil components and antibiotics: a review. Crit. Rev. Microbiol. 40, 76–94. https://doi.org/10.3109/1040841X.2013.763219.

Li, Y., Kong, D., Fu, Y., Sussman, M.R., Wu, H., 2020. The effect of developmental and environmental factors on secondary metabolites in medicinal plants. Plant Physiol. Biochem. 148, 80–89. https://doi.org/10.1016/j.plaphy.2020.01.006.

Lkhoumsi, D., Chafai, E.A., Guermal, A., Bachar, M., Boukil, M., 2004. Guide de Bonnes Pratiques de Collecte de Plantes Aromatiques et Médicinales du Maroc. Projet plantes médicinales et aromatiques.

Ma, C., Yu, L.J., Hassan, C.S., Elango, N., Tey, W.Y., Lai, G.N.Y., Chen, R.S., Tarawneh, M.A., 2023. Comparison of hydrodistillation for the extraction of essential oils from fruit peels with other methods. Chem. Eng. Trans. 106, 1141–1146. https://doi.org/10.3303/CET23106191.

Magaji, B., Singh, P., Skelton, A.A., Martincigh, B.S., 2023. Synthesis, photostability and antibacterial activity of a series of symmetrical α,β-unsaturated ketones as potential UV filters. J. Photochem. Photobiol. A: Chem. 445, 115018. https://doi.org/10.1016/j.jphotochem.2023.115018.

Manandhar, S., Singh, A., Varma, A., Pandey, S., Shrivastava, N., 2018. Evaluation of methods to detect *in vitro* biofilm formation by staphylococcal clinical isolates. BMC. Res. Notes. 11, 714. https://doi.org/10.1186/s13104-018-3820-9.

Messaoudi, M., Rebiai, A., Sawicka, B., Atanassova, M., Ouakouak, H., Larkem, I., Egbuna, C., Awuchi, C.G., Boubekeur, S., Ferhat, M.A., Begaa, S., Benchikha, N., 2022. Effect of extraction methods on polyphenols, flavonoids, mineral elements, and biological activities of essential oil and extracts of Mentha pulegium L. Molecules. 27, 11. https://doi.org/10.3390/molecules27010011.

Mollea, C., Bosco, F., Fissore, D., 2022. Agar plate methods for assessing the antibacterial activity of thyme and oregano essential oils against S. epidermidis and E. coli. Antibiotics. (Basel) 11, 1809. https://doi.org/10.3390/antibiotics11121809.

Morshdy, A.E.M.A., El-tahlawy, A.S., Qari, S.H., Qumsani, A.T., Bay, D.H., Sami, R., Althubaiti, E.H., Mansour, A.M.A., Aljahani, A.H., Hafez, A.E.-S.E., Mahmoud, A.F.A., El Bayomi, R.M., Hussein, M.A., 2022. Anti-biofilms' Activity of garlic and thyme essential oils against Salmonella typhimurium. Molecules. 27, 2182. https://doi.org/10.3390/molecules27072182.

Nurzynska-Wierdak, R., Zawislak, G., 2016. Chemical composition and antioxidant activity of lavender (Lavandula angustifolia Mill.) aboveground parts. Acta Scientiarum Polonorum. Hortorum Cultus 15.

Oualdi, I., Elfazazi, K., Azzouzi, H., Oussaid, A., Touzani, R., 2023. Chemical composition and antimicrobial properties of Moroccan Mentha pulegium L. essential oil. Mater. Today: Proc., Fifth Ed. Int. Conf. Mater. Environ. Sci. (ICMES 2022) 72, 3768–3774. https://doi.org/10.1016/j.matpr.2022.09.318.

Piechota, M., Kot, B., Frankowska-Maciejewska, A., Grużewska, A., Woźniak-Kosek, A., 2018. Biofilm formation by methicillin-resistant and methicillin-sensitive Staphylococcus aureus strains from hospitalized patients in Poland. Biomed. Res. Int., 4657396. https://doi.org/10.1155/2018/4657396 2018.

Pokajewicz, K., Białoń, M., Svydenko, L., Fedin, R., Hudz, N., 2021. Chemical composition of the essential oil of the new cultivars of Lavandula angustifolia Mill. Bred in Ukraine. Molecules. 26, 5681. https://doi.org/10.3390/molecules26185681.

Rafik, A., Abouddihaj, B., Asmaa, D., Kaotar, N., Mohammed, T., 2021. Antibiotic resistance profiling of uropathogenic Enterobacteriaceae, Casablanca, Morocco. E3S Web Conf 319, 01002. https://doi.org/10.1051/e3sconf/202131901002.

Ramzi, A., El Ouali Lalami, A., Ez zoubi, Y., Assouguem, A., Almeer, R., Najda, A., Ullah, R., Ercisli, S., Farah, A., 2022. Insecticidal effect of wild-grown Mentha pulegium and rosmarinus officinalis essential oils and their main monoterpenes against Culex pipiens (Diptera: Culicidae). Plants. (Basel) 11, 1193. https://doi.org/10.3390/plants11091193.

Rosato, A., Sblano, S., Salvagno, L., Carocci, A., Clodoveo, M.L., Corbo, F., Fracchiolla, G., 2020. Anti-biofilm inhibitory synergistic effects of combinations of essential oils and antibiotics. Antibiotics. (Basel) 9, 637. https://doi.org/10.3390/antibiotics9100637.

Sharma, A.D., Kaur, I., 2022. Aroma profile and in-silico molecular docking studies of essential oil against "aspergillosis" from *eucalyptus polybrachtea*. South African J. Botany 147, 754–763. https://doi.org/10.1016/j.sajb.2022.03.011.

Sreepian, A., Popruk, S., Nutalai, D., Phutthanu, C., Sreepian, P.M., 2022. Antibacterial activities and synergistic interaction of Citrus essential oils and limonene with Gentamicin against clinically isolated methicillin-resistant Staphylococcus aureus. ScientificWorldJournal., 8418287. https://doi.org/10.1155/2022/8418287 2022.

Walsh, D.J., Livinghouse, T., Goeres, D.M., Mettler, M., Stewart, P.S., 2019. Antimicrobial activity of naturally occurring phenols and derivatives against biofilm and planktonic bacteria. Front. Chem. 7.

Yakhlef, G., Hambaba, L., Pinto, D.C., Silva, A.M., 2020. Chemical composition and insecticidal, repellent and antifungal activities of essential oil of Mentha rotundifolia (L.) from Algeria. Ind. Crops Prod. Ind. Crops Products 158, 112988.

Yousefi, M., Pourmand, M.R., Fallah, F., Hashemi, A., Mashhadi, R., Nazari-Alam, A., 2016. Characterization of Staphylococcus aureus biofilm formation in urinary tract infection. Iran. J. Public Health 45, 485–493.